Chapter 2
Signals and Systems

It is a fact that signals and systems in feedback control are in continuous time and multivariable in nature. This is a contrast to data communications where the signals and systems are discrete time with single transmitter/receiver. But the wide use of digital computers in control systems and the emergence of wireless internet have diminished such differences between feedback control and data communications. Both are now in discrete time and both are MIMO systems. More importantly, they tend to use increasingly the same mathematical descriptions in modeling and share more and more mathematical tools in design. This text is aimed to provide the design theory and computational algorithms for MIMO dynamical systems in which either optimal disturbance rejection or optimal data detection is the main objective. This chapter introduces the background material for signals and systems.

Mathematical models are indispensable in design of both communication and control systems. To accommodate to data communications, signals are assumed to be discrete time and complex-valued. For MIMO systems, signals of interest are those having more than one component, each of which is random. Such signals are sequences of random vectors, assumed to be WSS, and have bounded power spectral densities (PSDs). Linear time-invariant (LTI) systems are capable of altering signals through modifying their PSDs in a transparent way. Commonly used dynamical models will be described and analyzed. LTV systems are also covered, albeit at a less degree. Although signals include noises in a larger sense, noise models will be discussed separately in this chapter, together with the bit error rate (BER) analysis in data communications.

2.1 Signals and Spectral Densities

For simplicity, the discrete-time variable t is measured in units of the sampling interval, and is thus integer-valued. That is, if $s(t)$ is a discrete-time signal obtained through sampling of the continuous-time signal $s_c(\cdot)$, then $s(t) = s_c(tT_s)$ for

G. Gu, *Discrete-Time Linear Systems: Theory and Design with Applications*,
DOI 10.1007/978-1-4614-2281-5_2,

$t = 0, \pm 1, \pm 2, \ldots$, with T_s the sampling period. In other words, a discrete-time signal can be viewed as a complex sequence $\{s(t)\}$ indexed by integer-valued time t.

2.1.1 Scalar Signals

Suppose that $\{s(t)\}$ is deterministic and has finite energy. Then

$$E_\mathrm{s} := \sum_{t=-\infty}^{\infty} |s(t)|^2 < \infty, \tag{2.1}$$

where E_s is the energy of $\{s(t)\}$. In this case, there exists DTFT for $\{s(t)\}$, defined as

$$S\left(\mathrm{e}^{j\omega}\right) := \sum_{t=-\infty}^{\infty} s(t)\mathrm{e}^{-j\omega t},\ j = \sqrt{-1}. \tag{2.2}$$

The corresponding inverse DTFT of $S\left(\mathrm{e}^{j\omega}\right)$ is given by

$$s(t) := \frac{1}{2\pi}\int_{-\pi}^{\pi} S\left(\mathrm{e}^{j\omega}\right)\mathrm{e}^{j\omega t}\,\mathrm{d}\omega. \tag{2.3}$$

The angular frequency $\omega = \omega_\mathrm{c} T_\mathrm{s}$ is normalized and measured in radians per sampling period where ω_c is the *physical frequency variable* measured in radians per second. Occasionally, $f = \omega/(2\pi)$ will be used, which has unit Hertz (Hz). If (2.1) holds, then by the well-known Parseval's theorem,

$$E_\mathrm{s} = \sum_{t=-\infty}^{\infty} |s(t)|^2 = \frac{1}{2\pi}\int_{-\pi}^{\pi} \left|S(\mathrm{e}^{j\omega})\right|^2\,\mathrm{d}\omega. \tag{2.4}$$

It follows that $\Phi_\mathrm{s}(\omega) = \left|S(\mathrm{e}^{j\omega})\right|^2$ represents the energy distribution of the sequence over frequency and is thus termed *energy spectral density* (ESD).

The ESD can be obtained through a different path. Define

$$\gamma_\mathrm{s}(k) = \sum_{t=-\infty}^{\infty} s(t)\bar{s}(t-k),\ k = 0, \pm 1, \pm 2, \ldots. \tag{2.5}$$

The sequence $\{\gamma(k)\}$ resembles autocovariance sequence for random signals. For any energy-bounded signals $\{x(t)\}$ and $\{y(t)\}$, there holds

$$\left|\sum_{t=-\infty}^{\infty} x(t)\bar{y}(t)\right| \le \sqrt{E_x E_y}, \tag{2.6}$$

which is the well-known Schwarz inequality. See Problem 2.2 in Exercises. Substituting $x(t) = s(t)$ and $y(t) = s(t-k)$ into (2.6) yields

$$E_s = \gamma_s(0) \geq \gamma_s(k) \text{ for } k = \pm 1, \pm 2, \ldots, \tag{2.7}$$

by noting $E_x = E_y = E_s$. Applying DTFT to $\{\gamma_s(k)\}$ yields

$$\begin{aligned} \sum_{k=-\infty}^{\infty} \gamma_s(k) e^{-j\omega k} &= \sum_{k=-\infty}^{\infty} \sum_{t=-\infty}^{\infty} \left[s(t) e^{-j\omega t} \right] \left[\bar{s}(t-k) e^{j\omega(t-k)} \right] \\ &= S\left(e^{j\omega}\right) S\left(e^{j\omega}\right)^* = \left| S(e^{j\omega}) \right|^2 = \Phi_s(\omega) \end{aligned}$$

with * for conjugate transpose. Hence, the ESD is the DTFT of the sequence $\{\gamma_s(k)\}$.

In engineering practice, signals are often described by their probabilistic statements and are thus random sequences. Such a signal sequence consists of an ensemble of possible realizations, each of which has some associated probability to occur. However, even if the signal is taken to be deterministic, which is one realization from the whole ensemble, it may not have finite energy over the infinite time horizon. In particular, signals in data communications do not possess DTFTs in general. On the other hand, a random signal usually has a finite average power and thus admits PSD.

Denote $\mathrm{E}\{\cdot\}$ as the expectation operator which averages over the ensemble of realizations. The discrete-time signal $\{s(t)\}$ is assumed to be a complex sequence of random variables, or *random process* with zero mean:

$$\mathrm{E}\{s(t)\} = 0, \; t = 0, \pm 1, \pm 2, \ldots. \tag{2.8}$$

If, in addition, its *ACS* is given by

$$r_s(k) := \mathrm{E}\{s(t)\bar{s}(t-k)\}, \; t = 0, \pm 1, \pm 2, \ldots, \tag{2.9}$$

which is independent of t, then $\{s(t)\}$ is called *WSS*. It is easy to see that $r_s(k) = \bar{r}_s(-k)$ and is left as an exercise to show that

$$r_s(0) \geq |r_s(k)| \text{ for } k = \pm 1, \pm 2, \ldots. \tag{2.10}$$

The PSD is defined as DTFT of ACS:

$$\Psi_s(\omega) := \sum_{k=-\infty}^{\infty} r_s(k) e^{-jk\omega}. \tag{2.11}$$

The inverse DTFT recovers $\{r_s(k)\}$ from the given $\Psi_s(\omega)$ via

$$r_s(k) = \frac{1}{2\pi} \int_{-\pi}^{\pi} \Psi_s(\omega) e^{j\omega k} \, \mathrm{d}\omega. \tag{2.12}$$

The averaged power of $\{s(t)\}$ is thus

$$P_{\rm s} := \mathrm{E}\left\{|s(t)|^2\right\} = r_{\rm s}(0) = \frac{1}{2\pi}\int_{-\pi}^{\pi} \Psi_{\rm s}(\omega)\,\mathrm{d}\omega, \tag{2.13}$$

which is also called mean-squared value of $s(t)$.

Example 2.1. Let ω_0 be real. Consider random signal

$$s(t) = A\cos(\omega_0 t + \Theta),\ 0 < \omega_0 < 2\pi, \tag{2.14}$$

where A and Θ are often employed to carry information bits in data communications. This example examines the case when A and Θ are real random variables, independent to each other, and uniformly distributed over $[0,\ 1]$ and $[0,\ 2\pi)$, respectively. The ensemble is a set of sinusoids with random amplitude and phase angle. Simple calculation shows

$$\begin{aligned}\mathrm{E}\{s(t)\} &= \mathrm{E}\{A\cos(\omega_0 t + \Theta)\}\\ &= \mathrm{E}\{A\cos(\omega_0 t)\cos(\Theta) - A\sin(\omega_0 t)\sin(\Theta)\}\\ &= \cos(\omega_0 t)\mathrm{E}\{A\}\mathrm{E}\{\cos(\Theta)\} - \sin(\omega_0 t)\mathrm{E}\{A\}\mathrm{E}\{\sin(\Theta)\} = 0,\end{aligned}$$

by independence, and $\mathrm{E}\{\cos(\Theta)\} = \mathrm{E}\{\sin(\Theta)\} = 0$. In addition,

$$\begin{aligned}\mathrm{E}\{s(t)\bar{s}(t-k)\} &= \mathrm{E}\left\{A^2\cos(\omega_0 t + \Theta)\cos(\omega_0(t-k) + \Theta)\right\}\\ &= \frac{1}{2}\mathrm{E}\left\{A^2\right\}\mathrm{E}\{\cos(\omega_0 k) + \cos(2\omega_0 t - \omega_0 k + 2\Theta)\}\\ &= \frac{1}{2}\mathrm{E}\left\{A^2\right\}\cos(\omega_0 k) = r_{\rm s}(k).\end{aligned}$$

It follows that $\{s(t)\}$ is WSS. By the hypothesis on A, $\mathrm{E}\{A^2\} = 1/3$. Thus,

$$\Psi_{\rm s}(\omega) = \frac{1}{6}\sum_{k=-\infty}^{\infty}\cos(\omega_0 k)\mathrm{e}^{-j\omega k} = \frac{1}{12}\left[\delta_D(\omega+\omega_0) + \delta_D(\omega-\omega_0)\right]$$

with $\delta_D(\cdot)$, the Dirac delta function, satisfying

$$\text{(i) } \delta_D(x) = 0 \text{ for } x \neq 0,\ \text{(ii) } \int_{\infty}^{\infty}\delta_D(x)\,\mathrm{d}x = 1. \tag{2.15}$$

The above indicates that there are two spectrum lines at $\pm\omega_0$, respectively. The analytical expression of $r_{\rm s}(k)$ is useful in computing PSD of $\{s(t)\}$.

In practice, there is a difficulty in evaluating the PSD as defined in (2.11). Infinitely, many terms need be computed for ACS, which is not feasible. An

approximate PSD is employed, consisting of finitely many signal samples:

$$\Psi_{\mathrm{s}}^{(n)}(\omega) = \mathrm{E}\left\{ \frac{1}{n} \left| \sum_{t=0}^{n-1} s(t) \mathrm{e}^{-j\omega t} \right|^2 \right\}. \tag{2.16}$$

A natural question is whether or not $\Psi_{\mathrm{s}}^{(n)}(\omega)$ converges to $\Psi_{\mathrm{s}}(\omega)$ as $n \to \infty$. By straightforward calculation,

$$\begin{aligned} \Psi_{\mathrm{s}}^{(n)}(\omega) &= \frac{1}{n} \sum_{t=0}^{n-1} \sum_{\tau=0}^{n-1} \mathrm{E}\{ s(t) \bar{s}(\tau) \} \mathrm{e}^{-j\omega(t-\tau)} \\ &= \sum_{k=-n}^{n} \left(1 - \frac{|k|}{n} \right) r_{\mathrm{s}}(k) \mathrm{e}^{-jk\omega}. \end{aligned}$$

Since multiplication in time domain is the same as convolution in frequency-domain, the above yields

$$\Psi_{\mathrm{s}}^{(n)}(\omega) = \frac{1}{2\pi} \int_{-\pi}^{\pi} F_n(\theta) \Psi_{\mathrm{s}}(\omega - \theta) \, \mathrm{d}\theta, \tag{2.17}$$

where $F_n(\omega)$ is the nth order *Fejér's kernel* given by

$$F_n(\omega) := \sum_{k=-n}^{n} \left(1 - \frac{|k|}{n} \right) \mathrm{e}^{-jk\omega} = \frac{1}{n} \left(\frac{\sin \frac{n}{2}\omega}{\sin \frac{1}{2}\omega} \right)^2. \tag{2.18}$$

Verification of the Fejér's kernel is left as an exercise (Problem 2.5). Before investigating the convergence issue for the approximate PSD in (2.17), it is illuminating to learn the useful properties of the Fejér's kernel.

Lemma 2.1. *Let $F_n(\omega)$ be defined as in (2.18). Then*

(i) $F_n(\omega) \geq 0 \ \forall \omega \in [0, 2\pi]$;
(ii) $\dfrac{1}{2\pi} \displaystyle\int_0^{2\pi} F_n(\omega) \, \mathrm{d}\omega = 1$ *for every* $n > 0$;
(iii) *For any closed interval* I *in* $(0, 2\pi)$, $\displaystyle\lim_{n\to\infty} \sup_{\omega \in \mathrm{I}} |F_n(\omega)| = 0$.

The proof of this lemma is again left as an exercise (Problem 2.5). The next theorem is the main result of this section.

Theorem 2.2. *Suppose that the random signal $\{s(t)\}$ has a finite averaged power. Then it admits the* PSD *as defined in (2.11). Let $\Psi_{\mathrm{s}}(\omega)$ be continuous over $[0, 2\pi)$ and $\Psi_{\mathrm{s}}(0) = \Psi_{\mathrm{s}}(2\pi)$. Define $\Psi_{\mathrm{s}}^{(n)}(\omega)$ as in (2.17). Then*

$$\lim_{n\to\infty} \Psi_{\mathrm{s}}^{(n)}(\omega) = \lim_{n\to\infty} \mathrm{E}\left\{ \frac{1}{n} \left| \sum_{t=0}^{n-1} s(t) \mathrm{e}^{-j\omega t} \right|^2 \right\} = \Psi_{\mathrm{s}}(\omega)$$

for all $\omega \in [0,\ 2\pi]$. *In other words,* $\Psi_{\mathrm{s}}^{(n)}(\omega)$ *converges uniformly to* $\Psi(\omega)$.

Proof. By the expression of $\Phi_{\mathrm{s}}^{(n)}(\omega)$ in (2.17) and (ii) of Lemma 2.1,

$$\Psi_{\mathrm{s}}^{(n)}(\omega) - \Psi_{\mathrm{s}}(\omega) = \frac{1}{2\pi} \int_{-\pi}^{\pi} [\Psi_{\mathrm{s}}(\omega - \theta) - \Psi_{\mathrm{s}}(\omega)] F_n(\theta)\, \mathrm{d}\theta.$$

Since $\Psi_{\mathrm{s}}(\omega)$ is a continuous function of ω, there exists an $M > 0$ such that $|\Psi_{\mathrm{s}}(\omega)| \le M$ for all $\omega \in [-\pi,\ \pi]$. Take $\delta > 0$ and write

$$\begin{aligned} \Psi_{\mathrm{s}}^{(n)}(\omega) - \Psi_{\mathrm{s}}(\omega) = {} & \frac{1}{2\pi} \int_{-\delta}^{\delta} [\Psi_{\mathrm{s}}(\omega - \theta) - \Psi_{\mathrm{s}}(\omega)] F_n(\theta)\, \mathrm{d}\theta \\ & + \frac{1}{2\pi} \int_{\delta \le |\theta| \le \pi} [\Psi_{\mathrm{s}}(\omega - \theta) - \Psi_{\mathrm{s}}(\omega)] F_n(\theta)\, \mathrm{d}\theta. \end{aligned}$$

It follows from Lemma 2.1 that

$$\left| \Psi_{\mathrm{s}}^{(n)}(\omega) - \Psi_{\mathrm{s}}(\omega) \right| \le \sup_{|\theta| \le \delta} |\Psi_{\mathrm{s}}(\omega - \theta) - \Psi_{\mathrm{s}}(\omega)| + 2M \sup_{\delta \le |\theta| \le \pi} F_n(\theta). \tag{2.19}$$

According to property (3) of Lemma 2.1, and by the continuity of $\Psi_{\mathrm{s}}(\omega)$, there exists an $N > 0$ such that for all $n \ge N$ and $\omega \in [0,\ 2\pi]$,

$$\left| \Psi_{\mathrm{s}}^{(n)}(\omega) - \Psi_{\mathrm{s}}(\omega) \right| \le \varepsilon$$

for any given $\varepsilon > 0$. Therefore, $\Psi_{\mathrm{s}}^{(n)}(\omega)$ converges uniformly to $\Psi_{\mathrm{s}}(\omega)$. □

There is no loss of generality in using only the causal part of the signal for approximate PSD $\Psi_{\mathrm{s}}^{(n)}(\omega)$ due to the WSS assumption for the random signal $\{s(t)\}$. In fact, (2.17) is also useful in the case when the PDF of $s(t)$ is unknown, in which case the PSD is often estimated using time averages instead of the ensemble average, by assuming ergodic process for $\{s(t)\}$. Since the measured signal data are always finitely many, they can be assumed to begin at time $t = 0$.

Theorem 2.2 reveals an important property of the PSD:

$$\Psi_{\mathrm{s}}(\omega) \ge 0 \ \ \forall\, \omega. \tag{2.20}$$

That is, PSDs are positive real functions of frequency, even though $\Psi_{\mathrm{s}}(\omega) = \Psi_{\mathrm{s}}(-\omega)$ may not hold in the case of complex signals. If the random signals are real, then there holds $\Psi_{\mathrm{s}}(\omega) = \Psi_{\mathrm{s}}(-\omega) \ge 0$ for all ω.

2.1.2 Vector Signals

For MIMO communication channels, the data signals are vector-valued, denoted by boldfaced letters, at each sampling time t. Consider the vector signal $\{\mathbf{s}(t)\}$ with size $p > 1$. If $\{\mathbf{s}(t)\}$ is deterministic, then it is assumed that the energy of the vector signal is bounded. That is,

$$E_{\mathbf{s}} := \sum_{t=-\infty}^{\infty} \|\mathbf{s}(t)\|^2 < \infty, \tag{2.21}$$

where $\|\mathbf{s}(t)\| = \sqrt{\mathbf{s}(t)^* \mathbf{s}(t)}$ is the Euclidean norm of $\mathbf{s}(t)$. In this case, the DTFT of $\{\mathbf{s}(t)\}$ exists and has the same expression as (2.2):

$$\mathbf{S}\left(\mathrm{e}^{j\omega}\right) := \sum_{t=-\infty}^{\infty} \mathbf{s}(t)\mathrm{e}^{-j\omega t}. \tag{2.22}$$

Define the $p \times p$ matrices

$$\Gamma_{\mathbf{s}}(k) = \sum_{t=-\infty}^{\infty} \mathbf{s}(t)\mathbf{s}(t-k)^*, \; k = 0, \pm 1, \pm 2, \ldots. \tag{2.23}$$

Although each term in the summation has rank one, $\Gamma_{\mathbf{s}}(k)$ may have a rank greater than one and even be nonsingular. Moreover, $\{\Gamma_{\mathbf{s}}(k)\}$ is a bounded matrix sequence. There holds

$$E_{\mathbf{s}} = \mathrm{Tr}\{\Gamma_{\mathbf{s}}(0)\} \geq |\mathrm{Tr}\{\Gamma_{\mathbf{s}}(k)\}| \text{ for } k = \pm 1, \pm 2, \ldots. \tag{2.24}$$

Similar to the scalar case, the ESD can be defined as the DTFT of $\{\Gamma_{\mathbf{s}}(k)\}$:

$$\Phi_{\mathbf{s}}(\omega) = \sum_{k=-\infty}^{\infty} \Gamma_{\mathbf{s}}(k)\mathrm{e}^{-j\omega k} = \mathbf{S}\left(\mathrm{e}^{j\omega}\right)\mathbf{S}\left(\mathrm{e}^{j\omega}\right)^*. \tag{2.25}$$

The above can be obtained with a similar derivation as in the scalar case. It is interesting to observe that $\Phi_{\mathbf{s}}(\omega)$ always has rank one for all ω, even though $\Gamma_{\mathbf{s}}(k)$ may have a rank greater than one for each k. Consequently,

$$\mathrm{Tr}\{\Phi_{\mathbf{s}}(\omega)\} = \mathrm{Tr}\left\{\mathbf{S}\left(\mathrm{e}^{j\omega}\right)\mathbf{S}(\mathrm{e}^{j\omega})^*\right\} = \mathbf{S}\left(\mathrm{e}^{j\omega}\right)^*\mathbf{S}\left(\mathrm{e}^{j\omega}\right) = \left\|\mathbf{S}(\mathrm{e}^{j\omega})\right\|^2,$$

by properties of the trace. Parseval's theorem is extended to

$$E_{\mathbf{s}} = \sum_{t=-\infty}^{\infty} \|\mathbf{s}(t)\|^2 = \frac{1}{2\pi}\int_{-\pi}^{\pi} \left\|\mathbf{S}(\mathrm{e}^{j\omega})\right\|^2 \, \mathrm{d}\omega. \tag{2.26}$$

For the case of random vector signals, it is assumed that $\{\mathbf{s}(t)\}$ is WSS with mean $\mathrm{E}\{\mathbf{s}(t)\} = \mathbf{0}_{\mathrm{p}}$ for all t. Then its ACS is given by

$$R_{\mathbf{s}}(k) := \mathrm{E}\{\mathbf{s}(t)\mathbf{s}(t-k)^*\},\ k = 0, \pm 1, \pm 2, \ldots, \tag{2.27}$$

which is independent of t and has size $p \times p$. Similar to the deterministic case, $R_{\mathbf{s}}(k)$ can be nonsingular. It can be shown that (Problem 2.7 in Exercises)

$$\text{(i)}\ R_{\mathbf{s}}(k)^* = R_{\mathbf{s}}(-k),\ \ \text{(ii)}\ \mathrm{Tr}\{R_{\mathbf{s}}(0)\} \geq |\mathrm{Tr}\{R_{\mathbf{s}}(k)\}|. \tag{2.28}$$

Assume that $R_{\mathbf{s}}(0)$ exists and is bounded. Then the PSD of $\{\mathbf{s}(t)\}$ can be easily extended from (2.11) via the DTFT of ACS:

$$\Psi_{\mathbf{s}}(\omega) := \sum_{k=-\infty}^{\infty} R_{\mathbf{s}}(k)\mathrm{e}^{-jk\omega}. \tag{2.29}$$

Different from the ESD in the deterministic case, the PSD $\Psi_{\mathbf{s}}(\omega)$ is nonsingular generically. The inverse DTFT recovers $\{R_{\mathbf{s}}(k)\}$ via

$$R_{\mathbf{s}}(k) = \frac{1}{2\pi}\int_{-\pi}^{\pi} \Psi_{\mathbf{s}}(\omega)\mathrm{e}^{j\omega k}\,\mathrm{d}\omega. \tag{2.30}$$

The averaged power of $\{\mathbf{s}(t)\}$ is generalized as follows:

$$P_{\mathbf{s}} := \mathrm{E}\{\mathbf{s}(t)^*\mathbf{s}(t)\} = \mathrm{Tr}\{R_{\mathbf{s}}(0)\} = \mathrm{Tr}\left\{\frac{1}{2\pi}\int_{-\pi}^{\pi} \Psi_{\mathbf{s}}(\omega)\,\mathrm{d}\omega\right\}. \tag{2.31}$$

Example 2.3. Consider random vector signal

$$\mathbf{s}(t) = A\mathbf{x}(t),\ \ \mathbf{x}(t) = \begin{bmatrix} \cos(\omega_0 t + \Theta) \\ \sin(\omega_0 t + \Theta) \end{bmatrix}, \tag{2.32}$$

where A and Θ are real independent random variables uniformly distributed over $[0,\ 1]$ and $[0,\ 2\pi)$, respectively, as in Example 2.1. It is easy to show that $\mathrm{E}\{\mathbf{s}(t)\} = \mathbf{0}$ and

$$\mathrm{E}\{\mathbf{x}(t)\mathbf{x}(t-k)^*\} = \frac{1}{2}\begin{bmatrix} \cos(\omega_0 k) & -\sin(\omega_0 k) \\ \sin(\omega_0 k) & \cos(\omega_0 k) \end{bmatrix} =: R_{\mathbf{x}}(k).$$

See Problem 2.6 in Exercises. Thus, by independence and $\mathrm{E}\{A^2\} = 1/3$,

$$\mathrm{E}\{\mathbf{s}(t)\mathbf{s}(t-k)^*\} = \mathrm{E}\{A^2\}\mathrm{E}\{\mathbf{x}(t)\mathbf{x}(t-k)^*\} = \frac{1}{6}\begin{bmatrix} \cos(\omega_0 k) & -\sin(\omega_0 k) \\ \sin(\omega_0 k) & \cos(\omega_0 k) \end{bmatrix}.$$

It follows that $\{\mathbf{s}(t)\}$ is WSS with $R_{\mathbf{s}}(k) = \mathrm{E}\{\mathbf{s}(t)\mathbf{s}(t-k)^*\}$ as above, which is nonsingular for all k. Direct calculation yields

$$\Phi_{\mathbf{s}}(\omega) = \frac{1}{6}\sum_{k=-\infty}^{\infty}\begin{bmatrix}\cos(\omega_0 k) & -\sin(\omega_0 k)\\ \sin(\omega_0 k) & \cos(\omega_0 k)\end{bmatrix}\mathrm{e}^{-j\omega k}$$
$$= \frac{1}{12}\left(\delta_D(\omega+\omega_0)\begin{bmatrix}1 & -j\\ j & 1\end{bmatrix} + \delta_D(\omega-\omega_0)\begin{bmatrix}1 & j\\ -j & 1\end{bmatrix}\right).$$

Thus, each element of the PSD matrix $\Psi_{\mathbf{s}}(\omega)$ contains two spectrum lines at $\pm\omega_0$, respectively, as in the scalar case. The power of the signal is given by $P_{\mathrm{s}} = \mathrm{Tr}\{R_{\mathbf{s}}(0)\} = 1/3$.

Approximate PSD can be employed if there are only finitely many terms of ACS available. The following

$$\Psi_{\mathbf{s}}^{(n)}(\omega) = \mathrm{E}\left\{\frac{1}{n}\left(\sum_{t=0}^{n-1}\mathbf{s}(t)\mathrm{e}^{-j\omega t}\right)\left(\sum_{\tau=0}^{n-1}\mathbf{s}(\tau)\mathrm{e}^{-j\omega\tau}\right)^*\right\} \tag{2.33}$$

is generalized from (2.16). Straightforward calculation gives

$$\Psi_{\mathbf{s}}^{(n)}(\omega) = \frac{1}{n}\sum_{t=0}^{n-1}\sum_{\tau=0}^{n-1}\mathrm{E}\{\mathbf{s}(t)\mathbf{s}(\tau)^*\}\mathrm{e}^{-j\omega(t-\tau)}$$
$$= \sum_{k=-n}^{n}\left(1-\frac{|k|}{n}\right)R_{\mathbf{s}}(k)\mathrm{e}^{-jk\omega}$$
$$= \frac{1}{2\pi}\int_{-\pi}^{\pi}F_n(\theta)\Psi_{\mathbf{s}}(\omega-\theta)\,\mathrm{d}\theta,$$

where $F_n(\cdot)$ is the nth order Fejér's kernel as defined in (2.18). Because Fejér's kernel is a scalar function, the matrix-valued ACS and PSD do not pose any difficulty in extending Theorem 2.2 to the following.

Theorem 2.4. *Suppose that the random vector signal* $\{\mathbf{s}(t)\}$ *has a finite averaged power. Then it admits the* PSD *as defined in (2.29). Let* $\Psi_{\mathbf{s}}(\omega)$ *be continuous over* $[0,\ 2\pi)$ *and* $\Psi_{\mathbf{s}}(0) = \Psi_{\mathbf{s}}(2\pi)$. *Define* $\Psi_{\mathbf{s}}^{(n)}(\omega)$ *as in (2.33). Then*

$$\lim_{n\to\infty}\Psi_{\mathbf{s}}^{(n)}(\omega) = \Psi_{\mathbf{s}}(\omega)\ \ \forall\ \omega\in[0,\ 2\pi].$$

Example 2.5. As an application example, consider estimation of the PSD based on a given set of N data samples $\{\mathbf{s}(t)\}_{t=0}^{N-1}$ in the absence of the statistical information of the underlying signal. To employ $\Psi_{\mathbf{s}}^{(n)}(\omega)$ in (2.33) as an approximation, it is assumed that $N = nm$ with n and m integers. The data set is partitioned into m disjoint subsets $\{\mathbf{s}_i(t)\}_{t=0}^{n-1}$, where $i = 0, 1, \ldots, m-1$. A simple partition is

$$\mathbf{s}_i(t) = \mathbf{s}(in+t),\ 0\le i\le m-1,\ 0\le t\le n-1.$$

Let $W_n = \mathrm{e}^{-j2\pi/n}$. For $i = 0, 1, \ldots, m-1$, compute

$$S_i(k) = \frac{1}{\sqrt{n}} \sum_{t=0}^{n-1} \mathbf{s}_i(t) W_n^{tk},\ k = 0, 1, \ldots, n-1, \tag{2.34}$$

which is a modified discrete Fourier transform (DFT). That is, it computes n frequency response samples uniformly distributed over $[0,\ 2\pi]$ for $\{\mathbf{s}_i(t)\}_{t=0}^{n-1}$ modified by a factor of $\frac{1}{\sqrt{n}}$. The FFT (fast Fourier transform) algorithm can be used to implement the computation in (2.34). Now the ensemble average in (2.33) at $\omega = \omega_k = \frac{2k\pi}{n}$ is replaced by the time average as follows:

$$\Psi^{(n)}(\omega_k) \approx \frac{1}{m} \sum_{i=0}^{m-1} S_i(k) S_i(k)^*,\ k = 0, 1, \ldots, n-1. \tag{2.35}$$

If $\{\mathbf{s}(t)\}$ is an ergodic process, the right-hand side converges to $\Psi^{(n)}(\omega_k)$ as $m \to \infty$, which in turn converges to the true PSD $\Psi(\omega)$ uniformly as $n \to \infty$. Theorem 2.4 is the basis for such a spectral estimation technique.

2.2 Linear Systems

Systems can be viewed as operators which map input signals to output signals according to some mathematical mechanisms. A linear system is a linear map whose output is a linear function of the input. This text focuses on LTI systems that provide transparent relations between spectral densities of the input signals and output signals. In fact, LTI systems shape the spectral densities of the input signals through a simple multiplicative operation capable of producing entirely different spectral densities at the output. LTV systems will also be studied in this section, albeit at a less degree.

2.2.1 Transfer Functions and Matrices

An LTI scalar system can be represented by its transfer function which is the $\mathscr{Z}$ transform of its impulse response, as illustrated below (see Fig. 2.1).

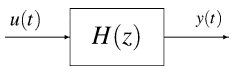

Fig. 2.1 An LTI system represented by its transfer function

That is, if $u(t) = \delta(t)$, which is the Kroneker delta function, then $y(t) = h(t)$ for $t = 0, \pm 1, \pm 2, \ldots$, with $\{h(t)\}$ the impulse response. The transfer function of the system is given by

$$H(z) := \sum_{t=-\infty}^{\infty} h(t) z^{-t},\ z \in \mathbb{C}. \tag{2.36}$$

For any input $\{u(t)\}$, the output of the system is the *convolution* of the impulse response with the input:

$$y(t) = h(t) \star u(t) := \sum_{k=-\infty}^{\infty} h(t-k) u(k). \tag{2.37}$$

The system is said to be causal, if $h(t) = 0$ for $t < 0$, and strictly causal, if $h(t) = 0$ for $t \leq 0$. Physical systems are causal in general, and often strictly causal. The following defines the notion of *stability*.

Definition 2.1. A system is said to be stable, if for every bounded input $\{u(t)\}$ (i.e., $|u(t)| \leq M_u < \infty$ for all t, and some $M_u > 0$), the corresponding output $\{y(t)\}$ is bounded (i.e., $|y(t)| \leq M_y < \infty$ for all t, and some $M_y > 0$).

The above stability is also termed BIBO (bounded-input/bounded-output) stability. The next result provides the stability criterion.

Theorem 2.6. *An* LTI *system with transfer function as in (2.36) is stable, if and only if*

$$\sum_{t=-\infty}^{\infty} |h(t)| < \infty. \tag{2.38}$$

Proof. For any bounded input $\{u(t)\}$ satisfying $|u(t)| \leq M_u < \infty$ for all t, and some $M_u > 0$, the output satisfies

$$|y(t)| = \left| \sum_{k=-\infty}^{\infty} h(t-k) u(k) \right| \leq \left(\sum_{k=-\infty}^{\infty} |h(k)| \right) M_u =: M_y < \infty$$

for $t = 0, \pm 1, \pm 2, \ldots$. Hence, (2.38) implies stability of the given LTI system. Conversely for the stable LTI system in (2.36), consider input $\{u(t)\}$ given by

$$u(k) = \begin{cases} \bar{h}(t_0 - k)/|h(t_0 - k)|, & h(t_0 - k) \neq 0, \\ 0, & h(t_0 - k) = 0, \end{cases}$$

with t_0 an integer. Then $|u(t)| \leq 1$ for all t and

$$y(t_0) = \sum_{k=-\infty}^{\infty} h(t_0 - k) u(k) = \sum_{k=-\infty}^{\infty} |h(t_0 - k)| = \sum_{t=-\infty}^{\infty} |h(t)| < \infty$$

by the stability assumption. Thus, stability implies (2.38). □

Notice that if the LTI system is both stable and causal, then

$$H(z) = \sum_{t=0}^{\infty} h(t) z^{-t} \tag{2.39}$$

is analytic at $z \in \mathbb{C}$ such that $|z| > 1$ and continuous on the unit circle. In other words, the region of convergence (ROC) is $|z| \geq 1$. In the interest of this text, only a subset of causal and stable LTI systems will be studied. This is the set of causal and stable LTI systems that admit rational transfer functions, or have finitely many poles and zeros. The causality of such a system is equivalent to the properness of its transfer function. Moreover, there exists a positive number $r < 1$ such that its ROC is $|z| > r$. That is, it is also analytic on the unit circle. Various system models will be presented in the next subsection.

For MIMO LTI systems, both input and output are vector signals. Capital letters, for example, $\{H(t)\}$, are used to denote impulse responses. The $\mathscr{Z}$ transform of the impulse response $\{H(t)\}$ is a transfer function matrix, or simply called transfer matrix, denoted by boldfaced capital letter and defined by

$$\mathbf{H}(z) := \sum_{t=-\infty}^{\infty} H(t) z^{-t}. \tag{2.40}$$

If the input signal $\{\mathbf{u}(t)\}$ has dimension m and the output signal $\{\mathbf{y}(t)\}$ has dimension p, then $\mathbf{H}(z)$ has size $p \times m$ for each $z \in \mathbb{C}$. The input and the output are again governed by the convolution relation:

$$\mathbf{y}(t) = H(t) \star \mathbf{u}(t) := \sum_{k=-\infty}^{\infty} H(t-k)\mathbf{u}(k). \tag{2.41}$$

A vector signal $\{\mathbf{s}(t)\}$ is said to be bounded, if $\|\mathbf{s}(t)\| \leq M_{\mathbf{s}}$ for all t and some bounded $M_{\mathbf{s}} > 0$. The stability notion in Definition 2.1 can be easily generalized to MIMO systems.

Definition 2.2. A MIMO system is said to be stable, if for every bounded input $\{\mathbf{u}(t)\}$, the corresponding output $\{\mathbf{y}(t)\}$ is bounded.

Note that for vector equation $\mathbf{w} = A\mathbf{v}$ with A a fixed matrix, $\|\mathbf{w}\|$ is a function of $\mathbf{v}$. Recall that $\|\cdot\|$ is the Euclidean norm. There holds

$$\sup_{\|\mathbf{v}\|=1} \|\mathbf{w}\| = \sup_{\|\mathbf{v}\|=1} \|A\mathbf{v}\| = \overline{\sigma}(A) \tag{2.42}$$

with $\overline{\sigma}(\cdot)$ the maximum singular value (refer to Appendix A). The next result is extended from Theorem 2.6 by noting the equality (2.42) and by the fact that there exists $\mathbf{v}_0$ with $\|\mathbf{v}_0\| = 1$ such that $\|A\mathbf{v}_0\| = \overline{\sigma}(A)$.

Theorem 2.7. *The* LTI *system with transfer matrix as in (2.40) is stable, if and only if*

$$\sum_{t=-\infty}^{\infty} \overline{\sigma}(H(t)) < \infty. \tag{2.43}$$

The proof is left as an exercise (Problem 2.20). For deterministic input signals, output signals are deterministic as well. The convolution in time domain is translated into multiplication in $\mathscr{Z}$-domain or frequency domain:

$$\mathbf{Y}(z) = \mathbf{H}(z)\mathbf{U}(z),\ \mathbf{Y}\left(\mathrm{e}^{j\omega}\right) = \mathbf{H}\left(\mathrm{e}^{j\omega}\right)\mathbf{U}\left(\mathrm{e}^{j\omega}\right). \tag{2.44}$$

Let $\boldsymbol{\Phi}_{\mathbf{u}}(\omega) = \mathbf{U}\left(\mathrm{e}^{j\omega}\right)\mathbf{U}\left(\mathrm{e}^{j\omega}\right)^*$ be the ESD of the input. Then

$$\boldsymbol{\Phi}_{\mathbf{y}}(\omega) = \mathbf{Y}\left(\mathrm{e}^{j\omega}\right)\mathbf{Y}\left(\mathrm{e}^{j\omega}\right)^* = \mathbf{H}\left(\mathrm{e}^{j\omega}\right)\boldsymbol{\Phi}_{\mathbf{u}}(\omega)\mathbf{H}\left(\mathrm{e}^{j\omega}\right)^* \tag{2.45}$$

is the ESD of the output. As such, the frequency response of the system shapes the ESD of the input. It is appropriate to define the energy norm:

$$\|\mathbf{s}\|_{\mathscr{E}} := \sqrt{E_{\mathbf{s}}} = \sqrt{\sum_{t=-\infty}^{\infty} \|\mathbf{s}(t)\|^2}. \tag{2.46}$$

In light of (2.44), the energy norm of the output is given by

$$\|\mathbf{y}\|_{\mathscr{E}} = \sqrt{\mathrm{Tr}\left\{\frac{1}{2\pi}\int_{-\pi}^{\pi} \mathbf{H}(\mathrm{e}^{j\omega})\boldsymbol{\Phi}_{\mathbf{u}}(\omega)\mathbf{H}(\mathrm{e}^{j\omega})^*\,\mathrm{d}\omega\right\}}. \tag{2.47}$$

Generically, $\|\mathbf{y}\|_{\mathscr{E}} \neq \|\mathbf{u}\|_{\mathscr{E}}$, if $\mathbf{H}(z) \neq I$. Thus, the energy norm serves as an indicator on the frequency-shaping effect of the system frequency response.

For random signals, their DTFT may not exist and thus (2.44) may not hold, if the input is a random signal. Suppose that the input $\{\mathbf{u}(t)\}$ is a WSS random process with zero means and $\{R_{\mathbf{u}}(k)\}$ as the ACS. Then $\{\mathbf{y}(t)\}$ is a random process with zero mean due to $\mathrm{E}\{\mathbf{u}(t)\} = 0$ for all t and

$$\mathrm{E}\{\mathbf{y}(t)\} = \sum_{k=-\infty}^{\infty} H(t-k)\mathrm{E}\{\mathbf{u}(k)\} = 0\ \forall\, t.$$

In fact, the output is also a WSS random process. Specifically,

$$\begin{aligned}\mathrm{E}\{\mathbf{y}(t)\mathbf{y}(t-k)^*\} &= \sum_{\alpha=-\infty}^{\infty}\sum_{\beta=-\infty}^{\infty} H(t-\alpha)\mathrm{E}\{\mathbf{u}(\alpha)\mathbf{u}(\beta)^*\}H(t-k-\beta)^* \\ &= \sum_{\alpha=-\infty}^{\infty}\sum_{\beta=-\infty}^{\infty} H(t-\alpha)R_{\mathbf{u}}(\alpha-\beta)H(t-k-\beta)^*.\end{aligned}$$

With variable substitution $\gamma = \alpha - \beta$, the above results in

$$\begin{aligned}\mathrm{E}\{\mathbf{y}(t)\mathbf{y}(t-k)^*\} &= \sum_{\beta=-\infty}^{\infty}\sum_{\gamma=-\infty}^{\infty} H(t-\beta-\gamma)R_{\mathbf{u}}(\gamma)H(t-\beta-k)^* \\ &= \sum_{\beta=-\infty}^{\infty} \tilde{R}_{\mathbf{y}}(t-\beta)H(t-\beta-k)^* \\ &= \sum_{\tau=-\infty}^{\infty} \tilde{R}_{\mathbf{y}}(\tau)H(\tau-k)^* = R_{\mathbf{y}}(k),\end{aligned}$$

which is independent of time t, where $\tilde{R}_{\mathbf{y}}(\tau) = H(\tau) \star R_{\mathbf{u}}(\tau)$ with $\tau = t - \beta$. Hence, it is concluded that the output of an LTI system is a WSS random process, provided that the input is. Let $\Psi_{\mathbf{u}}(\omega)$ be the PSD associated with input. Applying DTFT to the ACS of $\{\mathbf{y}(t)\}$ shows that the PSD of the output is given by (Problem 2.9 in Exercises)

$$\Psi_{\mathbf{y}}(\omega) = \mathbf{H}\left(\mathrm{e}^{j\omega}\right)\Psi_{\mathbf{u}}(\omega)\mathbf{H}\left(\mathrm{e}^{j\omega}\right)^*. \tag{2.48}$$

The resemblance of (2.48) to (2.45) is obvious, implying that LTI systems are capable of shaping the PSD of the input signal through multiplicative operations. The frequency response of the underlying system determines how much frequency shaping the system can exert to the input PSD. A useful measure is the power norm:

$$\|\mathbf{s}\|_{\mathscr{P}} = \sqrt{P_{\mathbf{s}}} = \sqrt{\mathrm{E}\{\|\mathbf{s}(t)\|^2\}} = \sqrt{\mathrm{Tr}\{R_{\mathbf{s}}(0)\}}. \tag{2.49}$$

Thus, the power norm of the output is

$$\|\mathbf{y}\|_{\mathscr{P}} = \sqrt{\mathrm{Tr}\left\{\frac{1}{2\pi}\int_{-\pi}^{\pi}\mathbf{H}(\mathrm{e}^{j\omega})\Psi_{\mathbf{u}}(\mathrm{e}^{j\omega})\mathbf{H}(\mathrm{e}^{j\omega})^*\,\mathrm{d}\omega\right\}}, \tag{2.50}$$

which indicates the shaping effect of the system frequency response to the input PSD. More investigation will be carried out in later sections. If the input is white noise with zero mean and identity covariance, i.e., $\Phi_{\mathbf{u}}(\mathrm{e}^{j\omega}) \equiv I$, then (2.49) provides one way to compute the system norm defined by

$$\|\mathbf{H}\|_2 := \sqrt{\mathrm{Tr}\left\{\frac{1}{2\pi}\int_{-\pi}^{\pi}\mathbf{H}(\mathrm{e}^{j\omega})\mathbf{H}(\mathrm{e}^{j\omega})^*\,\mathrm{d}\omega\right\}} = \sqrt{\mathrm{Tr}\left\{\sum_{t=-\infty}^{\infty}H(t)H(t)^*\right\}} \tag{2.51}$$

in light of the Parseval's theorem. Such a system norm is sometime called Frobenius norm of the system. A more general system norm is

$$\|\mathbf{H}\|_{\mathrm{p}} := \left[\frac{1}{2\pi}\int_{-\pi}^{\pi}\left(\sqrt{\mathrm{Tr}\{\mathbf{H}(\mathrm{e}^{j\omega})\mathbf{H}(\mathrm{e}^{j\omega})^*\}}\right)^p \mathrm{d}\omega\right]^{1/p}$$

for $1 \le p < \infty$, which reduces to $\|\mathbf{H}\|_2$ for $p = 2$.

Example 2.8. Consider the scalar system with transfer function

$$H(z) = K\left(1 - 2\cos(\omega_h)z^{-1} + z^{-2}\right) = K\left(z - \mathrm{e}^{j\omega_h}\right)\left(z - \mathrm{e}^{-j\omega_h}\right),$$

where K is a real constant gain. Simple calculations show that

$$\left|H(\mathrm{e}^{j\omega})\right| = 2|K|\sqrt{\left|\sin\left(\frac{\omega+\omega_h}{2}\right)\sin\left(\frac{\omega-\omega_h}{2}\right)\right|}$$

and $\|H\|_2 = 2|K|\sqrt{1+\cos^2(\omega_h)/2}$. If the input to the system is $u(t) = s(t)$ with $s(t)$ as given in Example 2.1, then the input PSD is

$$\Psi_u(\omega) = \frac{1}{12}\left[\delta_D(\omega+\omega_0) + \delta_D(\omega-\omega_0)\right].$$

In the scalar case, (2.48) reduces to $\Psi_y(\omega) = \left|H\left(\mathrm{e}^{j\omega}\right)\right|^2 \Psi_u(\omega)$, and thus,

$$\begin{aligned}\Psi_y(\omega) &= \frac{K^2}{3}\left|\sin\left(\frac{\omega+\omega_h}{2}\right)\sin\left(\frac{\omega-\omega_h}{2}\right)\right|\left[\delta_D(\omega+\omega_0) + \delta_D(\omega-\omega_0)\right] \\ &= \frac{K^2}{3}\left|\sin\left(\frac{\omega_0+\omega_h}{2}\right)\sin\left(\frac{\omega_0-\omega_h}{2}\right)\right|\left[\delta_D(\omega+\omega_0) + \delta_D(\omega-\omega_0)\right]\end{aligned}$$

is the output PSD. It follows that the amplitude of the two spectrum lines of the input PSD is shaped by the frequency response $H\left(\mathrm{e}^{j\omega}\right)$ at frequency ω_0. Indeed, if $\omega_h = \pm\omega_0$, then $\Psi_y(\omega) \equiv 0$ and there are no spectrum lines for the output PSD. On the other hand, if $\omega_h \neq \pm\omega_0$, the maximum amplitude of the two spectrum lines at the output is given by (with either $\omega_h = 0$, or $\omega_h = \pi$)

$$\frac{K^2}{3}\max\left\{\cos^2(\omega_0/2),\ \sin^2(\omega_0/2)\right\} \geq \frac{K^2}{6},$$

which can be large if the gain K is large.

2.2.2 System Models

The systems under consideration are causal and stable LTI systems, which have finitely many poles. Such systems form a *dense set* in the class of all causal and stable systems having continuous frequency responses. In other words, any causal and stable LTI system which admits continuous frequency response can be approximated arbitrarily well by a causal and stable LTI system which has

finitely many poles, provided that the number of poles is adequately large in light of Weierstrass Theorem from calculus. Such systems are also called *finite-dimensional* due to their finitely many poles and, more importantly, that they can be implemented or realized with finitely many arithmetic and delay operations. This subsection will provide a brief review of commonly used mathematical models for finite-dimensional LTI systems.

FIR or MA Models

For MIMO systems with m input and p output, the FIR model, also called transversal filter, refers to the transfer matrices of the form

$$\mathbf{H}(z) = \sum_{k=0}^{\ell} H(k) z^{-k}, \tag{2.52}$$

where $H(k)$ is a matrix of size $p \times m$ and is the impulse response at time $t = k$. In obtaining the impulse response of the system, the m impulse inputs need be applied one by one. The corresponding m output signals of size p can then be packed together column-wise to form $\{H(t)\}_{t=0}^{\ell}$. Since the impulse response dies out in finitely many samples, it acquires the name FIR (finite impulse response).

Consider the system with FIR model in (2.52). Let $\{\mathbf{u}(t)\}$ and $\{\mathbf{y}(t)\}$ be the associated input and output signals, respectively. Then

$$\mathbf{y}(t) = \sum_{k=0}^{\ell} H(k)\mathbf{u}(t-k) = \sum_{k=t-\ell}^{t} H(t-k)\mathbf{u}(k). \tag{2.53}$$

That is, the output is the (weighted) moving average (MA) of the input. Hence, the input/output description in (2.53) for the FIR model is also called the MA model. FIR or MA models are the simplest, yet extremely important, for wireless communication systems. The wireless channels are characterized by multipath, of which gains of each path can be regarded as the impulse responses of the channels and are often complex valued.

IIR or ARMA Models

The IIR model for SISO systems has the fractional form

$$H(z) = \frac{N(z)}{M(z)} = \frac{\nu_0 + \nu_1 z^{-1} + \cdots + \nu_{n_\nu} z^{-n_\nu}}{1 - \mu_1 z^{-1} - \cdots - \mu_{n_\mu} z^{-n_\mu}}, \tag{2.54}$$

where $\mu_k \neq 0$ for at least one integer $k > 0$ and $M(z) \neq 0$ for all z outside and on the unit circle. It follows that the system is stable and has a causal and infinite impulse

response (IIR). Let $\{u(t)\}$ and $\{y(t)\}$ be the associated input and output signals, respectively. Then

$$y(t) = \sum_{k=1}^{n_\mu} \mu_k y(t-k) + \sum_{k=0}^{n_\nu} \nu_k u(t-k). \tag{2.55}$$

That is, the output $y(t)$ consists of two parts: the autoregressive (AR) part in the first summation and the MA part in the second summation. If $\nu_k = 0$ for $k = 1, 2, \ldots, n_\nu$, then the ARMA model reduces to the AR model, in which case the system admits an all-pole model. Hence, the ARMA model includes the AR model as a special case. In light of (2.55), the computational complexity in computing the output $y(t)$ is dependent on the degrees of the numerator and denominator polynomials in the ARMA model (2.54). There is an incentive to minimize n_ν and n_μ, which can be carried out through cancelation of the common factors or common roots of $M(z)$ and $N(z)$. If $M(z)$ and $N(z)$ do not share common roots, then $\{M(z), N(z)\}$ is called *relative coprime* or simply *coprime*. In this case, the roots of $N(z)$ are called *zeros*, the roots of $M(z)$ are called *poles*, and $n = \max\{n_\nu, n_\mu\}$ is called the *degree* of the system.

For MIMO systems with m input and p output, the transfer matrices for the IIR model can be extended to the left fractional form

$$\mathbf{H}(z) = \mathbf{M}(z)^{-1}\mathbf{N}(z) = \left(M_0 - \sum_{k=1}^{n_\mu} M_k z^{-k}\right)^{-1} \left(\sum_{k=0}^{n_\nu} N_k z^{-k}\right), \tag{2.56}$$

where M_k is a $p \times p$ matrix and N_k is a $p \times m$ matrix for each integer k. Again, $M_k \neq \mathbf{0}_{p\times p}$ for at least one integer $k > 0$, assuming M_0 is nonsingular. If M_0 is an identity, then the following describes the MIMO ARMA model:

$$\mathbf{y}(t) = \sum_{k=1}^{n_\mu} M_k \mathbf{y}(t-k) + \sum_{k=0}^{n_\nu} N_k \mathbf{u}(t-k), \tag{2.57}$$

where $\{\mathbf{u}(t)\}$ and $\{\mathbf{y}(t)\}$ are the input and output signals, respectively. For MIMO systems, there exists right fractional form

$$\mathbf{H}(z) = \tilde{\mathbf{N}}(z)\tilde{\mathbf{M}}(z)^{-1} = \left(\sum_{k=0}^{\tilde{n}_\nu} \tilde{N}_k z^{-k}\right) \left(\tilde{M}_0 - \sum_{k=1}^{\tilde{n}_\mu} \tilde{M}_k z^{-k}\right)^{-1}, \tag{2.58}$$

which can be entirely different from the one in (2.56).

Several notions need be introduced for MIMO systems. For the left fraction in (2.56), $\{\mathbf{M}(z), \mathbf{N}(z)\}$ is called left coprime, if

$$\operatorname{rank}\{[\,\mathbf{M}(z)\ \mathbf{N}(z)\,]\} = p \quad \forall\, z \in \mathbb{C}. \tag{2.59}$$

For the right fraction in (2.58), $\{\tilde{\mathbf{N}}(z), \tilde{\mathbf{M}}(z)\}$ is called right coprime, if

$$\operatorname{rank}\left\{\begin{bmatrix}\tilde{\mathbf{M}}(z)\\ \tilde{\mathbf{N}}(z)\end{bmatrix}\right\} = m \quad \forall\, z \in \mathbb{C}. \tag{2.60}$$

In practice, it is unnecessary to test the rank conditions in (2.59) and (2.60) at all $z \in \mathbb{C}$. For the left fraction, one needs test (2.59) only at those z which are roots of $\det(\mathbf{M}(z)) = 0$, and in the case of the right fraction, one needs test (2.60) only at those z which are roots of $\det\left(\tilde{\mathbf{M}}(z)\right) = 0$.

Suppose that $\{\mathbf{M}(z), \mathbf{N}(z)\}$ and $\{\tilde{\mathbf{N}}(z), \tilde{\mathbf{M}}(z)\}$ are left and right coprimes, respectively. A complex number p_0 is called pole of $\mathbf{H}(z)$, if:

$$\lim_{z\to p_0} \operatorname{rank}\{\mathbf{M}(z)\} < p \iff \lim_{z\to p_0} \operatorname{rank}\{\tilde{\mathbf{M}}(z)\} < m. \tag{2.61}$$

That is, some elements of $\mathbf{H}(z)$ become unbounded as $z \to p_0$. A complex number z_0 is called zero of $\mathbf{H}(z)$, if with $\rho = \min\{p, m\}$,

$$\lim_{z\to z_0} \operatorname{rank}\{\mathbf{N}(z)\} < \rho \iff \lim_{z\to z_0} \operatorname{rank}\{\tilde{\mathbf{N}}(z)\} < \rho. \tag{2.62}$$

That is, $\operatorname{rank}\{\mathbf{H}(z)\} < \rho = \min\{p, m\}$ as $z \to z_0$. The system is stable, if $\mathbf{H}(z)$ has all its poles strictly inside the unit circle. The system is called *minimum phase*, if $\mathbf{H}(z)$ has no zeros outside the unit circle, and called *strict minimum phase*, if $\mathbf{H}(z)$ has no zeros on and outside the unit circle.

Example 2.9. For systems with single input ($m = 1$), their right coprime fractions can be easily obtained, which amounts to computing the greatest common divisor (GCD). Specifically, consider the case of $p = 2$ with

$$\begin{aligned}\mathbf{H}(z) = \tilde{\mathbf{N}}(z)\tilde{M}(z)^{-1} &= \begin{bmatrix}a_1 + b_1 z^{-1} + c_1 z^{-2}\\ a_2 + b_2 z^{-1} + c_2 z^{-2}\end{bmatrix}\left(1 - \alpha z^{-1} - \beta z^{-2}\right)^{-1}\\ &= \begin{bmatrix}a_1\left(1 - s_{1,1}z^{-1}\right)\left(1 - s_{1,2}z^{-1}\right)\\ a_2\left(1 - s_{2,1}z^{-1}\right)\left(1 - s_{2,2}z^{-1}\right)\end{bmatrix}\left[\left(1 - p_1 z^{-1}\right)\left(1 - p_2 z^{-1}\right)\right]^{-1}.\end{aligned}$$

The system has a zero at z_o, if and only if $z_o \neq p_1$, $z_o \neq p_2$, and $z_o = s_{1,i} = s_{2,k}$ for some i and k. The right coprimeness condition in (2.60) is equivalent to whether or not the two numerator and one denominator polynomials have common roots. Thus, $\{\tilde{\mathbf{N}}(z), \tilde{M}(z)\}$ is not right coprime, if and only if

$$\begin{aligned}\mathbf{H}(z) &= \begin{bmatrix}a_1\left(1 - s_1 z^{-1}\right)\\ a_2\left(1 - s_2 z^{-1}\right)\end{bmatrix}\frac{\left(1 - s z^{-1}\right)}{\left(1 - s z^{-1}\right)\left(1 - p z^{-1}\right)}\\ &= \begin{bmatrix}a_1\left(1 - s_1 z^{-1}\right)\\ a_2\left(1 - s_2 z^{-1}\right)\end{bmatrix}\frac{1}{1 - p z^{-1}},\end{aligned}$$

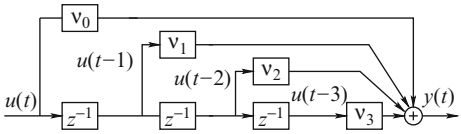

Fig. 2.2 Block diagram for FIR models of degree $n = 3$

for some s. If $\left(1 - sz^{-1}\right)$ is the GCD, then the last expression of the above equation provides a right coprime fraction, which has a zero if and only if $s_1 = s_2$. This procedure can be easily generalized to other single input systems. As a result, the procedure for obtaining the right coprime fractions for single-input systems is quite similar to that for SISO systems, which can be extended to compute the left coprime fractions for single output ($p = 1$) systems.

It is possible for $\mathbf{H}(z)$ to have common poles and zeros while its fractions are coprime. Generically, it is difficult to obtain coprime fractions for MIMO systems, and coprime fractions are not possible, if $M_0 = I_{\mathrm{p}}$ and $\tilde{M}_0 = I_m$ are required. Consequently, it is considerably more difficult to minimize the computational complexity associated with the right-hand side of (2.57) than the case of SISO systems. For this and other reasons, state-space models are more preferred for MIMO systems to be discussed next.

State-Space Models

State-space models describe dynamic systems with *state variables*. Let FIR models of degree 3 be realized as in the following block diagram.

Then the input/output relation in Fig. 2.2 satisfies (2.55) for $n = n_v = 3$ and $\mu_k = 0 \ \forall \ k \geq 1$. A common practice in the state-space description is to take the output of each delay device as the state variable. Thus, for the SISO MA model, one may define $n = n_v$ state variables $\{x_k(t)\}_{k=1}^{n}$ via

$$\mathbf{x}(t) = \begin{bmatrix} x_1(t) \\ x_2(t) \\ \vdots \\ x_n(t) \end{bmatrix} = \begin{bmatrix} u(t-1) \\ u(t-2) \\ \vdots \\ u(t-n) \end{bmatrix} \implies \mathbf{x}(t+1) = \begin{bmatrix} u(t) \\ x_1(t) \\ \vdots \\ x_{n-1}(t) \end{bmatrix}. \tag{2.63}$$

Let $d = v_0$. Then the state-space equations

$$\mathbf{x}(t+1) = A\mathbf{x}(t) + \mathbf{b}u(t), \ y(t) = \mathbf{c}\mathbf{x}(t) + du(t) \tag{2.64}$$

hold, where $(A, \mathbf{b}, \mathbf{c}, d)$ is called a *realization* of the system, given by

$$A = \begin{bmatrix} \mathbf{0}_{n-1}^{*} & 0 \\ I_{n-1} & \mathbf{0}_{n-1} \end{bmatrix}, \ \mathbf{b} = \begin{bmatrix} 1 \\ \mathbf{0}_{n-1} \end{bmatrix}, \ \mathbf{c} = \begin{bmatrix} v_1 & \cdots & v_n \end{bmatrix}, \tag{2.65}$$

in light of (2.63). The vector space spanned by state vectors $\mathbf{x}(t)$ at different time t is called state space and is determined by the pair $(A, \mathbf{b})$.

For the IIR model or ARMA model, it is assumed that

$$H(z) = d + \frac{\tilde{\nu}_1 z^{-1} + \tilde{\nu}_2 z^{-2} + \cdots + \tilde{\nu}_n z^{-n}}{1 - \mu_1 z^{-1} - \cdots - \mu_n z^{-n}}, \tag{2.66}$$

where $n = \max\{n_\nu, n_\mu\}$. The conversion from (2.54) to (2.66) is always possible by zero-padding either the AR coefficients or MA coefficients. In this case, $H(z)$ admits a realization $(A, \mathbf{b}, \mathbf{c}, d)$ with

$$A = \begin{bmatrix} \mathbf{v}_{n-1} & \mu_n \\ I_{n-1} & \mathbf{0}_{n-1} \end{bmatrix}, \ \mathbf{b} = \begin{bmatrix} 1 \\ \mathbf{0}_{n-1} \end{bmatrix}, \ \mathbf{c} = \begin{bmatrix} \tilde{\nu}_1 & \cdots & \tilde{\nu}_n \end{bmatrix}, \tag{2.67}$$

where $\mathbf{v}_{n-1} = \begin{bmatrix} \mu_1 & \cdots & \mu_{n-1} \end{bmatrix}$. The above is termed *canonical controller form* or simply *controller form*. To verify that $(A, \mathbf{b}, \mathbf{c}, d)$ is indeed a realization for $H(z)$ in (2.66), denote $\{x_k(t)\}$ as the corresponding state variables. Then for $1 \le k < n$,

$$x_{k+1}(t+1) = x_k(t) \implies x_k(t) = x_1(t-k+1).$$

Hence, for $d = 0$, the expressions in (2.67) and (2.64) yield

$$\begin{aligned} x_1(t+1) &= \sum_{k=1}^{n} \mu_k x_k(t) + u(t) = \sum_{k=1}^{n} \mu_k x_1(t-k+1) + u(t), \\ y(t) &= \sum_{k=1}^{n} \tilde{\nu}_k x_k(t) = \sum_{k=1}^{n} \tilde{\nu}_k x_1(t-k+1). \end{aligned}$$

Applying $\mathscr{Z}$ transform to the above with zero initial conditions yields

$$\begin{aligned} X_1(z) &= \frac{z^{-1} U(z)}{1 - \mu_1 z^{-1} - \cdots - \mu_n z^{-n}}, \\ Y(z) &= \left(\tilde{\nu}_1 + \tilde{\nu}_2 z^{-1} + \cdots + \tilde{\nu}_n z^{-n+1}\right) X_1(z), \end{aligned}$$

which verifies that the transfer function from $u(t)$ to $y(t)$ is indeed $H(z)$.

For MIMO FIR systems, a simple realization (A, B, C, D) is given by

$$\begin{aligned} A &= \begin{bmatrix} \mathbf{0}_{m\times(n-m)} & \mathbf{0}_{m\times m} \\ I_{(n-m)m} & \mathbf{0}_{(n-m)\times m} \end{bmatrix}, \ B = \begin{bmatrix} I_m \\ \mathbf{0}_{(n-m)\times m} \end{bmatrix}, \\ C &= \begin{bmatrix} H_1 & H_2 & \cdots & H_\ell \end{bmatrix}, \qquad D = H_0, \ n = m\ell, \end{aligned} \tag{2.68}$$

which is generalized from (2.65) and termed block controller form. Extension of the above realization to include the IIR MIMO system in (2.56) is left as an exercise (Problem 2.23). Its state-space system is described by

$$\mathbf{x}(t+1) = A\mathbf{x}(t) + B\mathbf{u}(t), \ \mathbf{y}(t) = C\mathbf{x}(t) + D\mathbf{u}(t), \tag{2.69}$$

where A, B, C and D have appropriate dimensions. Applying $\mathscr{Z}$ transform to (2.69) with zero initial condition $\mathbf{x}(0) = \mathbf{0}_n$ yields the transfer matrix

$$\mathbf{H}(z) = D + C(zI_n - A)^{-1}B. \tag{2.70}$$

Its impulse response $\{H(t)\}$ is given by

$$H(0) = D,\ H(t) = CA^{t-1}B,\ t \geq 1. \tag{2.71}$$

State-space realizations are not unique. For the state-space equation (2.69), let the linear transform be $\mathbf{x}_T(t) = T\mathbf{x}(t)$ with T square and nonsingular. Then $\mathbf{x}(t) = T^{-1}\mathbf{x}_T(t)$, which upon substituted into (2.69), yields

$$\mathbf{x}_T(t+1) = TAT^{-1}\mathbf{x}_T(t) + TBu(t),\ y(t) = CT^{-1}\mathbf{x}_T(t) + Du(t). \tag{2.72}$$

Hence, a different realization $\left(TAT^{-1}, TB, CT^{-1}, D\right)$ is obtained for the same system. The transform in (2.72) is called *similarity transform*. Since T is an arbitrary nonsingular matrix, a system can have infinitely many different realizations. Moreover, realizations with different state dimensions may exist. Minimal realizations are preferred due to the obvious reason of complexity. The dimension of the state vector $\mathbf{x}(t)$ is called *order* of the state-space system. If the order n is minimum among all possible realizations for the same system, then (A, B, C, D) is called a *minimal* realization.

Let p_0 be a pole of $\mathbf{H}(z)$. Then it is an eigenvalue of A. The converse may not be true in general unless the realization is minimal. Let z_0 be a zero of $\mathbf{H}(z)$. Then

$$\operatorname{rank}\left\{\begin{bmatrix} A - z_0 I_n & B \\ C & D \end{bmatrix}\right\} < n + \min\{p, m\}. \tag{2.73}$$

Again, the converse holds for only minimal realizations in general. The state-space system (2.69) is said to be internally stable, if all eigenvalues of A are strictly inside the unit circle. A formal definition for stability will be delayed to the next chapter. It is worth pointing out that the stability notion for state-space systems is stronger than the stability notion for ARMA models or transfer functions and matrices. The two coincide with each other when the state-space system has a minimal realization.

Example 2.10. The following transfer function

$$H(z) = \frac{-3z^{-1} + 6z^{-2}}{1 - 2z^{-1}} = \frac{-3z + 6}{z^2 - 2z} \tag{2.74}$$

admits a realization $(A, \mathbf{b}, \mathbf{c}, d)$ with

$$A = \begin{bmatrix} 2 & 0 \\ 1 & 0 \end{bmatrix},\ \mathbf{b} = \begin{bmatrix} 1 \\ 0 \end{bmatrix},\ \mathbf{c} = \begin{bmatrix} -3 & 6 \end{bmatrix},\ d = 0.$$

The state-space system is unstable as A has two eigenvalues with one at 2 and the other at 0. In absence of the input, the recursive computation yields

$$\mathbf{x}(t+1) = \begin{bmatrix} x_1(t+1) \\ x_2(t+1) \end{bmatrix} = A\mathbf{x}(t) = \begin{bmatrix} 2 \\ 1 \end{bmatrix} x_1(t) = \begin{bmatrix} 2^{t+1} \\ 2^t \end{bmatrix} x_1(0)$$

with $x_1(0)$ the first component of $\mathbf{x}(0)$. Hence, if $x_1(0) \neq 0$, each element of $\mathbf{x}(t)$ diverges as $t \to \infty$. On the other hand,

$$y(t) = \mathbf{c}\mathbf{x}(t) = \begin{bmatrix} -3 & 6 \end{bmatrix} \mathbf{x}(t) = -3 \times 2^t + 6 \times 2^{t-1} = 0.$$

So the unstable mode 2^t does not show up at the output. Alternatively, $H(z)$ in (2.74) admits a different realization with

$$A = \begin{bmatrix} 2 & 1 \\ 0 & 0 \end{bmatrix}, \ \mathbf{b} = \begin{bmatrix} -3 \\ 6 \end{bmatrix}, \ \mathbf{c} = \begin{bmatrix} 1 & 0 \end{bmatrix}, \ d = 0.$$

Again, A has eigenvalues at 2 and 0. Moreover, $x_1(t) = 2^t x_1(0) - 3u(t)$ and $y(t) = x_1(t)$ based on the recursive state-space equation. In this case, the unstable mode 2^t does show up at the output, but cannot be removed from both $x_1(t)$ and $x_2(t)$, i.e., stabilized by any bounded control input $\{u(t)\}$.

It is important to note $H(z) = -3z^{-1}$ after canceling the common factor $(z-2)$. Thus, the system is BIBO stable. The unstable eigenvalue at 2 is not a pole of $H(z)$. In fact, a minimal realization of $H(z)$ is $(A, \mathbf{b}, \mathbf{c}, d) = (0, 1, -3, 0)$, which is stable, coinciding with the stability of $H(z)$. This example illustrates a serious issue in realizations: It is possible for a system to be internally unstable while being externally or BIBO stable. Such realizations are harmful in the sense that unstable modes of the state-space system are either not detectable via the measured output or not stabilizable via the control input, which will be investigated thoroughly in the next chapter.

To summarize, the LTI models can be basically classified into two categories. The first one includes FIR or MA and IIR or ARMA models, which emphasizes input/output descriptions for dynamic systems. Its advantages lie in the simplicity and clear notions of poles, zeros, and stability. Such models are well studied for SISO systems. However, the coprime fractions for MIMO systems such as ARMA or IIR models are not easy to obtain, especially if $M_0 = I_p$ or $\tilde{M}_0 = I_m$ is required. The second category is the state-space models, which provide internal descriptions for dynamic systems in terms of state vectors. The dynamic behavior of the system is completely specified by the state variables and the input. Although more parameters are used, minimal realizations are always possible. Thus, poles, zeros, and stability can be characterized as well. More importantly, state-space models reveal internal structural information of the underlying systems and introduce new concepts and results for system design, which are especially suitable to MIMO systems. Hence, this text will focus on state-space models.

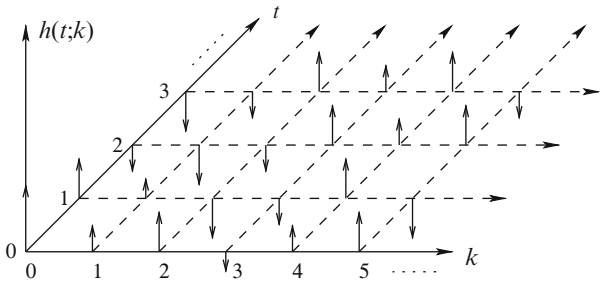

Fig. 2.3 Impulse response for SISO LTV systems

2.2.3 Time-Varying Systems

A LTV system can be viewed as a family of LTI systems parameterized by the time index t. As such, its impulse response is denoted by $\{h(t;k)\}$. Basically, $\{h(t_0;k)\}$ is an impulse response of the system at time t_0 with the impulse input applied at $k=0$. An illustrative plot is shown in Fig. 2.3. At each integer-valued time t, $h(t;k)$ is shown horizontally from left to right. For MIMO systems, impulse responses are denoted by $\{H(t;k)\}$. Let $\{\mathbf{u}(t)\}$ and $\{\mathbf{y}(t)\}$ be the input and output, respectively. Then

$$\mathbf{y}(t) = H(t;k) \star \mathbf{u}(t) = \sum_{k=-\infty}^{\infty} H(t;t-k)\mathbf{u}(k) = \sum_{k=-\infty}^{\infty} H(t,k)\mathbf{u}(k). \tag{2.75}$$

In the control literature, $H(t,k) = H(t;t-k)$ is the standard notation. If the impulse responses are all the same at different time index t, then (2.75) becomes the same as in (2.41) for LTI systems (see Fig. 2.3).

For LTV systems, transfer functions or transfer matrices do not exist. As a consequence, notions of poles and zeros are lost, and frequency-domain analysis is inapplicable, which are negative. On the positive side, the BIBO stability condition can be derived in a similar way to that for LTI systems, as shown in the following result.

Theorem 2.11. *The LTV system with impulse response $\{H(t;k)\}$ is BIBO stable, if and only if*

$$\sum_{k=-\infty}^{\infty} \overline{\sigma}(H(t;k)) < \infty, \quad \forall\, t. \tag{2.76}$$

Basically, the stability condition in Theorem 2.11 treats the LTV impulse response as a "frozen time" LTI system indexed by time t. Thus, its proof is similar to that for LTI systems and is left as an exercise (Problem 2.26). While the stability condition for LTV systems is simple and resembles that for LTI systems, difficulties exist to apply it in practice due to the lack of analytic form of $\{H(t;k)\}$ and verification of (2.76) for each t. It needs to be pointed out that for causal LTV systems, $H(t;k) = \mathbf{0}$ for $k < 0$, which is assumed in the rest of this subsection.

As shown earlier, outputs of LTI systems are WSS processes, provided that the inputs are also. However, this statement does not hold for LTV systems, even though $\mathrm{E}\{\mathbf{u}(t)\} = \mathbf{0}$ for all time t implies $\mathrm{E}\{\mathbf{y}(t)\} = \mathbf{0}$ for all t, in light of (2.75). Indeed, for white noise input with the identity covariance, the power of the output is time dependent and given by

$$\begin{aligned} P_{\mathbf{y}}(t) &= \mathrm{Tr}\left(\mathrm{E}\left\{\sum_{k=-\infty}^{t}\sum_{i=-\infty}^{t} H(t;t-k)\mathbf{u}(k)\mathbf{u}(i)^* H(t;t-i)^*\right\}\right) \\ &= \mathrm{Tr}\left\{\sum_{k=-\infty}^{t} H(t;t-k)H(t;t-k)^*\right\} = \mathrm{Tr}\left\{\sum_{k=0}^{\infty} H(t;k)H(t;k)^*\right\}. \quad (2.77) \end{aligned}$$

Basically, $P_{\mathbf{y}}(t)$ quantifies the energy of the impulse response at time t. The above suggests that the system norm in (2.51) for LTI systems be generalized to LTV systems as

$$\|\mathbf{H}_t\|_2 = \sqrt{\mathrm{Tr}\left\{\sum_{k=0}^{\infty} H(t;k)H(t;k)^*\right\}} \quad (2.78)$$

which is time dependent.

Even though LTV systems are considerably more difficult to analyze, MA, ARMA, and state-space models are still effective for the class of systems emphasized in this text. Specifically, the ARMA model in (2.57) for MIMO systems can be adapted to

$$\mathbf{y}(t) = -\sum_{k=1}^{n_\mu} M_k(t)\mathbf{y}(t-k) + \sum_{k=0}^{n_\nu} N_k(t)\mathbf{u}(t-k), \quad (2.79)$$

where the AR and MA coefficient matrices are function of time t. If $M_k(t) = 0$ for $1 \le k \le n_\mu$ and all time t, then the above is collapsed to the MA model

$$\mathbf{y}(t) = \sum_{k=0}^{n_\nu} N_k(t)\mathbf{u}(t-k)$$

and $\{N_k(t)\}$ can be viewed as an impulse response of the LTV system at time t. That is, $\{H(t,k) = N_k(t)\}$ is parameterized by time index t. It is noted that MA models, time varying or not, are always stable.

For state-space descriptions, state-space models are adapted to

$$\mathbf{x}(t+1) = A_t\mathbf{x}(t) + B_t\mathbf{u}(t),\ \mathbf{y}(t) = C_t\mathbf{x}(t) + D_t\mathbf{u}(t), \quad (2.80)$$

where (A_t, B_t, C_t, D_t) can be viewed as a realization for the underlying MIMO system at time t. For LTV MA models, a realization with time-invariant A can be used. But for general LTV systems, a time-varying A_t needs to be assumed. Similarity transform can also be applied to obtain a new realization $\left(TA_tT^{-1}, TB_t, C_tT^{-1}, D_t\right)$

for the same system, where T is square and nonsingular. If a time-varying nonsingular matrix T_t is used as transform, then similarity $\left(T_{t+1}A_tT_t^{-1}, T_{t+1}B_t, C_tT_t^{-1}, D_t\right)$ is a new realization.

Different from LTI systems, a clear relation is lacking between the impulse response $\{H(t;k)\}$ and the realization (A_t, B_t, C_t, D_t). Hence, "frozen time" analysis as in Theorem 2.11 cannot be used to study stability for LTV state-space systems. In fact, the stability notion for LTI state-space models is generalized to the following.

Definition 2.3. The state-space system (2.80) is said to be exponentially stable, if there exist some α and β with $\alpha > 0$ and $0 < \beta < 1$ such that

$$\rho\left(A_{t+N}A_{t+N-1}\cdots A_{t+1}A_t\right) \le \alpha\beta^N$$

for all time t and $N > 0$, where $\rho(\cdot)$ denotes the spectral radius.

In general, stability for each A_t, i.e., $\rho(A_t) < 1$ for each t, does not ensure stability of the state-space system (refer to Problem 2.27 in Exercises). It is worth to pointing out that if the state-space system is exponentially stable, then the state response to zero input with initial condition $\mathbf{x}(t_0) \neq \mathbf{0}_n$ is given by

$$\mathbf{x}(T) = \left(A_{t_0+T-1}A_{t_0+T-2}\cdots A_{t_0+1}A_{t_0}\right)\mathbf{x}(t_0) \to \mathbf{0}_n$$

for any $\mathbf{x}(t_0) \neq \mathbf{0}_n$, as $T \to \infty$. It is noted that in the case $A_t = A$ for all t, exponential stability reduces to the known condition that all eigenvalues of A are strictly inside the unit circle.

2.3 Noise Processes and BER Analysis

One of the impediments to data detection is the contamination of random noises at the receiver site. In most situations, observation noises can be assumed to be additive, white, and Gaussian noise (AWGN). Consider the signal model as illustrated below (see Fig. 2.4).

Let $\{\mathbf{v}(t)\}$ be AWGN. Then for each time index t, $\mathbf{v}(t)$ is a Gaussian random vector, i.e., $\mathbf{v}(t)$ is normal distributed. It is assumed that $\mathrm{E}[\mathbf{v}(t)] = \mathbf{0}$ for all t. The white assumption implies that the autocovariance matrix is given by

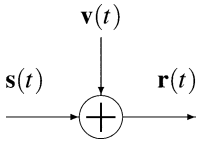

Fig. 2.4 Observed signal with contaminated noise

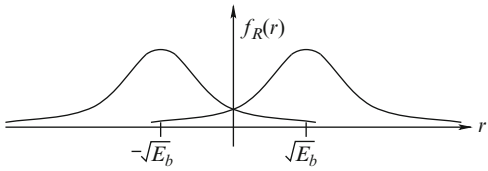

Fig. 2.5 PDF for received signal

$$\mathrm{E}\{\mathbf{v}(t)\mathbf{v}(t-k)^*\} = R_{\mathbf{v}}(t)\delta(k) = \begin{cases} R_{\mathbf{v}}(t), & \text{if } k=0, \\ 0, & \text{if } k\neq 0. \end{cases} \tag{2.81}$$

If $R_{\mathbf{v}}(t) \equiv R_{\mathbf{v}}$ is a constant nonnegative matrix, then the AWGN $\{\mathbf{v}(t)\}$ is WSS. Otherwise, the AWGN is nonstationary.

For the simple case of scalar signals and noises, $s(t) = \pm\sqrt{E_\mathrm{b}}$ and $v(t)$ is a Gaussian random variable with zero mean and variance σ_v^2. That is, $s(t)$ carries only one bit of information which is either $+1$ or -1, and E_b is the bit energy of $s(t)$. The data detection problem aims to detect the sign of $s(t)$ based on the observed signal $r(t)$ at each time index t. Clearly, $r(t)$ is also a Gaussian random variable and has PDF

$$f_R(r) = \frac{1}{\sqrt{2\pi}\sigma_v}\exp\left\{-\frac{(r-s)^2}{2\sigma_v^2}\right\},$$

where the time index t is skipped due to the stationarity of $s(t)$ and $v(t)$. The figure below shows the PDFs of the received signal $r(t)$ for both $s(t) = \sqrt{E_\mathrm{b}}$ and $s(t) = -\sqrt{E_\mathrm{b}}$. Note that there is a symmetry about $r(t) = 0$ (see Fig. 2.5).

For the case of equal probable $s(t)$, i.e., $s(t)$ takes equal number of positive and negative values, a moment of reflection indicates that the optimal detection rule is

$$\check{s}(t) = \begin{cases} +1, & \text{if } r(t) > 0, \\ -1, & \text{if } r(t) < 0. \end{cases} \tag{2.82}$$

Indeed, by symmetry, the probability of the BER is given by

$$\begin{aligned} \varepsilon_\mathrm{b} &= \int_0^\infty \frac{1}{\sqrt{2\pi}\sigma_v}\exp\left\{-\frac{(r+\sqrt{E_\mathrm{b}})^2}{2\sigma_v^2}\right\}\mathrm{d}r \\ &= \int_{\sqrt{E_\mathrm{b}/\sigma_v^2}}^\infty \frac{1}{\sqrt{2\pi}}\exp\left\{-\frac{r^2}{2}\right\}\mathrm{d}r =: Q\left(\sqrt{E_\mathrm{b}/\sigma_v^2}\right) \end{aligned} \tag{2.83}$$

that is the minimum. The quantity E_b/σ_v^2 is called signal-to-noise ratio (SNR). It is important to observe that the BER performance is determined solely by the SNR. Large SNR implies small BER and vice versa. If $s(t)$ is taken to be random, then E_b needs be replaced by bit power $P_\mathrm{b} = \mathrm{E}\{|s(t)|^2\}$.

The case when $s(t)$ carries more than one bit information is not pursued in this text due to two reasons. First, any data can be represented by binary codes. There is

no loss of generality in investigating the case of binary data. Second, generalization from binary data to the case of multiple bits does not involve new concepts and knowledge for data detection. Focusing on the binary case will help illuminate the basic issues and the essential difficulties and understand the approaches to optimal data detection.

For vector signals of size m, the noise $\mathbf{v}(t)$ is again assumed to be AWGN with mean zero and covariance $\Sigma_{\mathbf{v}}$. Suppose that $\Sigma_{\mathbf{v}}$ is nonsingular. Then the observed signal $\mathbf{r}(t)$ admits Gaussian distribution with PDF

$$f_R(\mathbf{r}) = \frac{1}{\sqrt{(2\pi)^m \det(\Sigma_{\mathbf{v}})}} \exp\left\{-\frac{1}{2}(\mathbf{r}-\mathbf{s})^* \Sigma_{\mathbf{v}}^{-1}(\mathbf{r}-\mathbf{s})\right\}. \tag{2.84}$$

Let $s_i(t)$ and $r_i(t)$ be the ith component of $\mathbf{s}(t)$ and $\mathbf{r}(t)$, respectively. For the equal probable case, the detection rule (2.82) can be adapted to

$$\breve{s}_i(t) = \begin{cases} +1, & \text{if} \quad r_i(t) > 0, \\ -1, & \text{if} \quad r_i(t) < 0, \end{cases} \qquad 1 \le i \le m. \tag{2.85}$$

Unfortunately, the above detection rule is not optimal anymore. The reason lies in the correlation of the noise components. For instance, the detected symbol, if correct, may help to detect other symbols. This problem will be studied in Chap. 7. Assume temporarily that $\Sigma_{\mathbf{v}}$ is diagonal. With $P_{\mathrm{s}}(i) = \mathrm{E}\left\{|s_i(t)|^2\right\}$ and $\sigma_{\mathbf{v}}^2(i) = \mathrm{E}\left\{|v_i(t)|^2\right\}$ (the ith diagonal element of $\Sigma_{\mathbf{v}}$), the corresponding BER is given by

$$\varepsilon_{\mathrm{b}}(i) = Q\left(P_{\mathrm{s}}(i)/\sigma_{\mathbf{v}}^2(i)\right), \ i = 1, 2, \ldots, m, \tag{2.86}$$

under the detection rule (2.85) where $Q(\cdot)$-function is defined as in (2.83). The average BER for detection of $\mathbf{s}(t)$ can be calculated according to

$$\overline{\varepsilon}_{\mathrm{b}} = \frac{1}{m}\sum_{i=1}^{m} Q\left(P_{\mathrm{s}}(i)/\sigma_{\mathbf{v}}^2(i)\right). \tag{2.87}$$

Gauss noise is a legitimate assumption in data communications, but the white assumption may not be, due to frequency-selective fading and the presence of the receiver. A common hypothesis is that the noise $\mathbf{v}(t)$, if colored, is generated by an LTI filter driven by a Gaussian white noise process $\mathbf{w}(t)$ of zero mean and identity covariance. That is, the PSD of $\mathbf{v}(t)$ is given by

$$\Psi_{\mathbf{v}}(\omega) = \mathbf{G}(\mathrm{e}^{j\omega})\Psi_{\mathbf{w}}(\omega)\mathbf{G}(\mathrm{e}^{j\omega})^*, \ \Psi_{\mathbf{w}}(\omega) \equiv I,$$

where $\mathbf{G}(z)$ can be assumed to be stable and minimum phase without loss of generality. It should be clear that the transmitted signal at the receiver site is also distorted, giving rise to the following signal model for data detection in Fig. 2.6.

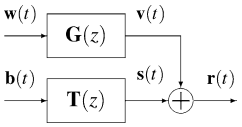

Fig. 2.6 Baseband signal model for data detection

This signal model is quite general in which $\mathbf{b}(t)$ is the original binary data signal at the transmitter, and $\mathbf{w}(t)$ is the AWGN with zero vector mean and identity covariance. The transfer matrices $\mathbf{T}(z)$ and $\mathbf{G}(z)$ are both causal, stable, and rational. Assume that $\mathbf{b}(t)$ and $\mathbf{s}(t)$ have the same size $m > 1$. Then

$$\mathbf{r}(t) = \mathbf{b}(t) + [T(t) - \delta(t)I_m] \star \mathbf{b}(t) + G(t) \star \mathbf{w}(t), \tag{2.88}$$

where $\{T(t)\}$ and $\{G(t)\}$ are impulse responses of $\mathbf{T}(z)$ and $\mathbf{G}(z)$, respectively. Even though $\mathbf{v}(t) = G(t) \star \mathbf{w}(t)$ can be treated as Gaussian distributed, the second term on the right-hand side of (2.88) does not have a normal distribution, in general.

Denote $D(t) = T(t) - \delta(t)I_m$ and $\mathbf{d}(t) = D(t) \star \mathbf{b}(t)$. Let $D_{i,\ell}(t)$ denote the (i,ℓ)th element of $D(t)$ and $d_i(t)$ the ith element of $\mathbf{d}(t)$. Then

$$d_i(t) = \sum_{k=-\infty}^{t} \sum_{\ell=1}^{m} D_{i,\ell}(k) b_\ell(t-k), \ 1 \le i \le m, \tag{2.89}$$

where $b_\ell(t)$ is the ℓth element of $\mathbf{b}(t)$, assumed to be equal probable and independent with respect to both ℓ and t. As such, one may conjecture that $\{d_i(t)\}$ is Gaussian distributed for each i by the *central limit theorem*. Unfortunately, it is not. The main reason is stability and rationality of $\mathbf{T}(z)$, two good properties as entailed for data communications, which imply the existence of $M > 0$ such that $|d_i(t)| \le M < \infty$ for all i and t by the boundedness of the input $\mathbf{b}(t)$. It follows that the support of PDF for $d_i(t)$ in (2.89) is finite precluding it from having normal distribution.

Although $\{\mathbf{d}(t)\}$ does not have a Gaussian distribution, it is close to being normal distributed, provided that impulse response $\{D(t)\}$ or equivalently $\{T(t)\}$ does not die out too quickly. Otherwise, m, the size of the data vector, needs to be adequately large. The next example illustrates this fact.

Example 2.12. Let Z be a random variable generated via

$$Z = \sum_{k=0}^{n-1} \rho^k Y_k, \ \rho = 0.8, \ n = 50,$$

where $\{Y_k\}$ is an i.i.d. sequence with an equal probability of 0.5 at ± 1. Clearly, Z has a zero mean and a variance

$$\mathrm{E}\left\{|Z|^2\right\} = \sum_{k=0}^{n-1} \rho^{2k} \mathrm{E}\left\{|Y_k|^2\right\} = \sum_{k=0}^{n-1} \rho^{2k} \le \frac{1}{1-\rho^2} = \frac{1}{0.36}.$$

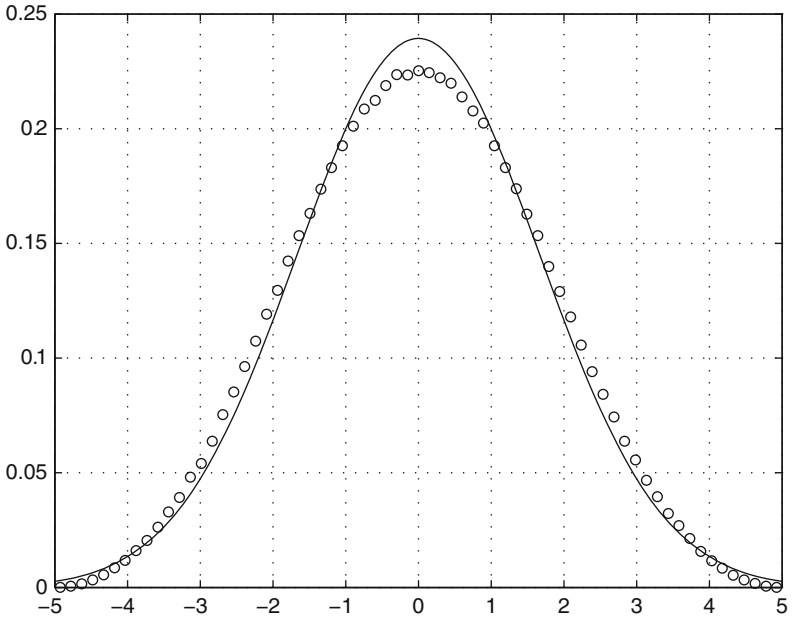

Fig. 2.7 Approximate PDF compared with normal distribution

One million samples of Z are obtained with Matlab, which produce an approximate PDF in Fig. 2.7, plotted with "o," based on the periodogram method. It can be observed that the curve is close to the Gaussian PDF with zero mean and variance $\frac{1}{0.36}$, plotted in solid line.

The aforementioned discussions are summarized next.

Proposition 2.1. *Suppose that* $\mathbf{G}(z)$ *and* $\mathbf{T}(z)$ *as in Fig. 2.6 are causal, stable, and rational. Let* $\{\mathbf{w}(t)\}$ *be AWGN of mean zero and covariance identity and* $\{\mathbf{b}(t)\}$ *be equal probable and independent. Denote* $\mathbf{D}(z) = \mathbf{T}(z) - I_m$ *and* $\Sigma_{\mathbf{b}} = \mathrm{E}\{\mathbf{b}(t)\mathbf{b}(t)^*\}$. *If the impulse response of* $\mathbf{D}(z)$ *does not die out too quickly or the size of the data vector is adequately large, then the observed signal* $\mathbf{r}(t)$ *in Fig. 2.6 consists of two parts: the transmitted data signal* $\mathbf{b}(t)$ *and a fictitious additive noise* $\{\mathbf{n}(t)\}$ *which has an approximate normal distribution with mean vector zero and covariance*

$$\Sigma_{\mathbf{n}} = \frac{1}{2\pi}\int_{-\pi}^{\pi}\left[\mathbf{G}\left(\mathrm{e}^{j\omega}\right)\mathbf{G}\left(\mathrm{e}^{j\omega}\right)^* + \mathbf{D}\left(\mathrm{e}^{j\omega}\right)\Sigma_{\mathbf{b}}\mathbf{D}\left(\mathrm{e}^{j\omega}\right)^*\right]\mathrm{d}\omega. \tag{2.90}$$

In light of (2.88), the fictitious additive noise is given by

$$\mathbf{n}(t) = D(t) \star \mathbf{b}(t) + G(t) \star \mathbf{w}(t)$$

with $D(t) = T(t) - \delta(t)I_m$. Its covariance matrix $\Sigma_{\mathbf{n}}$ can be computed according to (2.90) by the fact that $\{\mathbf{b}(t)\}$ and $\{\mathbf{w}(t)\}$ are independent of each other. Even

though $\{\mathbf{n}(t)\}$ is approximately Gaussian with zero vector mean, the detection rule in (2.85) cannot be used for data detection with $\hat{s}_i(t)$ replaced by $\hat{b}_i(t)$. There are two reasons. The first one is the poor SNR in terms of the new noise $\mathbf{n}(t)$, considering that $\mathbf{D}(z) = \mathbf{T}(z) - I$ has large power norm in absence of equalization or precoding. The second one is the nonwhite nature for $\{\mathbf{n}(t)\}$ and its dependence on $\mathbf{b}(t)$ in general. But if the SNR is high and the PSD is near flat for the new noise $\mathbf{n}(t)$, then the detection rule in (2.85) is approximately optimal. In this case, $\{\mathbf{n}(t)\}$ is close to being normal distributed, the formulas in (2.86) and (2.87) can be employed to estimate approximate BER values with $P_{\mathbf{s}}(i)$ replaced by $P_{\mathbf{b}}(i)$ and $\sigma_{\mathbf{v}}(i)$ by $\sigma_{\mathbf{n}}(i)$, which are the ith diagonal elements of $\Sigma_{\mathbf{b}}$ and $\Sigma_{\mathbf{n}}$, respectively. It is worth pointing out that, if $\mathbf{T}(z)$ and $\mathbf{G}(z)$ in Fig. 2.6 are replaced by time-varying systems with impulse responses $\{T(t,k)\}$ and $\{G(t,k)\}$, respectively, then the covariance in (2.90) is time dependent and given by:

$$\Sigma_{\mathbf{n}}(t) = \sum_{k=0}^{\infty} [G(t;k)G(t;k)^* + D(t;k)\Sigma_{\mathbf{b}}D(t;k)^*] \tag{2.91}$$

with $D(t,k) = T(t,k) - \delta(k)I_m$ in light of (2.77).

BER is the most important performance indicator for data detection, but it can be difficult to minimize in design of optimal receivers. It can also be difficult to compute, if the detection error does not have normal distribution. As shown earlier, the BER is hinged to the error variance, if the signal power is kept constant. For this reason, a closely related performance indicator, root-mean-squared error (RMSE), is often employed for data detection, which does not require the knowledge of distribution of the noise, provided that the PDF of the noise is symmetric about the origin. For the case in Proposition 2.1, the RMSE is simply $\varepsilon_{\mathrm{p}} = \sqrt{\mathrm{Tr}\{\Sigma_{\mathbf{n}}\}}$, i.e.,

$$\varepsilon_{\mathrm{p}} = \sqrt{\mathrm{Tr}\left\{\frac{1}{2\pi}\int_{-\pi}^{\pi}\left[\mathbf{G}\left(\mathrm{e}^{j\omega}\right)\mathbf{G}\left(\mathrm{e}^{j\omega}\right)^* + \mathbf{D}\left(\mathrm{e}^{j\omega}\right)\Sigma_{\mathbf{b}}\mathbf{D}\left(\mathrm{e}^{j\omega}\right)^*\right]\, d\omega\right\}}. \tag{2.92}$$

A receiver design algorithm that achieves the minimum RMSE is called minimum mean-squared-error (MMSE) algorithm. Although the RMSE performance is different from the BER performance, they are closely related. In the case of Gaussian processes, they are equivalent to each other in the sense that the detection rule remains the same. Data detection is often carried out after equalization or precoding which will be studied in Chap. 7.

Notes and References

Many books provide excellent coverage of signals and systems in the case of discrete-time. A sample of such textbooks are [7, 8, 69, 90, 100]. The BER analysis is based on textbooks for digital communications such as [92, 116].

Exercises

2.1. Prove (2.4) by assuming that $\{s(t)\}$ is deterministic and has finite energy.

2.2. Prove the Schwarz inequality (2.6).

2.3. Compute ESD for the discrete-time signal

$$s(t) = \mathrm{e}^{-\alpha|t|}\cos(\omega_0 t + \pi/2),\ \alpha > 0,\ \omega_0 \neq 0.$$

Compute energy of $\{s(t)\}$ in both time domain and frequency domain.

2.4. Let $\{r_s(k)\}$ be ACS of $\{s(t)\}$ as defined in (2.9). Show that for each integer k, $|r_s(k)| \leq r_s(0)$.

2.5. Verify the expression of the nth order Fejér's kernel in (2.18) and prove Lemma 2.1. (*Hint:* Note that for deterministic $\{s(t)\}$,

$$\Psi^{(n)}(\omega) = \frac{1}{n}\left|\sum_{t=0}^{n-1} s(t)\mathrm{e}^{-j\omega t}\right|^2$$

which is the same as $F_n(\omega)$ for $s(t) \equiv 1$).

2.6. Suppose that Θ is a uniformly distributed random variable over $[0,\ 2\pi]$. Show that

(a) $\mathrm{E}\{\cos^2(\Theta)\} = \mathrm{E}\{\sin^2(\Theta)\} = \frac{1}{2}$,
(b) $\mathrm{E}\{\cos(\Theta)\} = \mathrm{E}\{\sin(\Theta)\} = \mathrm{E}\{\cos(\Theta)\sin(\Theta)\} = 0$, and
(c) for $\mathbf{x}(t) = \big[\cos(\omega_0 t + \Theta)\ \sin(\omega_0 t + \Theta)\big]'$,

$$R_{\mathbf{x}}(k) = \mathrm{E}\{\mathbf{x}(t)\mathbf{x}(t-k)^*\} = \frac{1}{2}\begin{bmatrix}\cos(\omega_0 k) & -\sin(\omega_0 k)\\ \sin(\omega_0 k) & \cos(\omega_0 k)\end{bmatrix}.$$

2.7. Let $\{R_{\mathbf{s}}(k)\}$ be ACS of the WSS vector process $\{\mathbf{s}(t)\}$ as defined in (2.27). Show that for each integer k,

$$\text{(i) } R_{\mathbf{s}}(k)^* = R_{\mathbf{s}}(-k), \quad \text{(ii) } \mathrm{Tr}\{R_{\mathbf{s}}(0)\} \geq |\mathrm{Tr}\{R_{\mathbf{s}}(k)\}|.$$

(*Hint:* Note that $\mathrm{Tr}\{R_{\mathbf{s}}(0)\} = \mathrm{E}\{\mathbf{s}(t)^*\mathbf{s}(t)\} = \mathrm{E}\{\mathbf{s}(t-k)^*\mathbf{s}(t-k)\}$, and $|\mathrm{Tr}\{R_{\mathbf{s}}(k)\}| = |\mathrm{E}\{\mathbf{s}(t-k)^*\mathbf{s}(t)\}| = |\mathrm{E}\{\mathbf{s}(t)^*\mathbf{s}(t-k)\}|$, as well as

$$\mathrm{E}\left\{\begin{bmatrix}\mathbf{s}(t)^*\\ \mathbf{s}(t-k)^*\end{bmatrix}\big[\mathbf{s}(t)\ \mathbf{s}(t-k)\big]\right\} \geq \mathbf{0}$$

for each integer k).

2.8. For Example 2.3, set $\omega_0 = 0.25\pi$. Use Simulink to generate a set of $N = 2^{14}$ data samples for $\{\mathbf{s}(t)\}$ in (2.32):

1. Follow the estimation scheme outlined in Example 2.5 with $n = 2^8$ and $m = 2^6$ to estimate the PSD with comparison to the true PSD.
2. Consider the use of $\omega_0 = 0.25\pi + \pi/n$ with different values of (n,m), but with $N = nm = 2^{14}$ and the same data samples set. Compare the estimation results with that in (i).

The quantity π/n is called resolution in spectrum estimation which is the possible maximum error for the location of the spectrum lines.

2.9. Consider the system in Fig. 2.1. Let

$$r_{yu}(k) = \mathrm{E}\{y(t)u(t-k)^*\}$$

be the cross covariance sequence and $\Psi_{yu}(\omega)$ be the DTFT of $\{r_{yu}(k)\}$. Let $\Psi_u(\omega)$ and $\Psi_y(\omega)$ be the DTFT of ACS $\{r_u(k)\}$ and $\{r_y(k)\}$, respectively. Show that

$$\Psi_{yu}(\omega) = H\left(\mathrm{e}^{j\omega}\right)\Psi_u(\omega),\ \Psi_y(\omega) = \Psi_{yu}(\omega)H\left(\mathrm{e}^{j\omega}\right)^*.$$

Generalize the above to MIMO systems.

2.10. Let $\{y(t)\}_{t=0}^{n-1}$ and $\{u(t)\}_{t=0}^{n-1}$ be input and output measurement data. Approximate $r_{yu}(k)$ as in the previous problem by

$$\hat{r}_{yu}(k) = \begin{cases} \dfrac{1}{n}\displaystyle\sum_{t=k}^{n-1} y(t)u(t-k)^*, & k \geq 0, \\ \dfrac{1}{n}\displaystyle\sum_{t=0}^{n+k-1} y(t)u(t-k)^*, & k \leq 0. \end{cases}$$

Show that the DTFT of $\{\hat{r}_{yu}(k)\}$ is given by

$$\hat{\Psi}_{yu}(\omega) = \frac{1}{n}\left(\sum_{t=0}^{n-1} y(t)\mathrm{e}^{-jt\omega}\right)\left(\sum_{k=0}^{n-1} u(k)\mathrm{e}^{-jk\omega}\right)^*.$$

2.11. For the system in Fig. 2.1, propose an algorithm to estimate the system frequency response $\left|H(\mathrm{e}^{j\omega})\right|$ and $\angle H(\mathrm{e}^{j\omega})$. (*Hint:* Use the results in Problems 2.8, 2.9, and 2.10).

2.12. For the block diagram in Fig. 2.8, the block with L is an interpolator or upper sampler where $L > 1$ is an integer. The output of the interpolator is governed by

$$s(t) = \begin{cases} u(k), & \text{if } t = Lk, \\ 0, & \text{if } t \neq Lk. \end{cases}$$

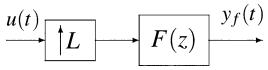

Fig. 2.8 Interpolator followed by filter

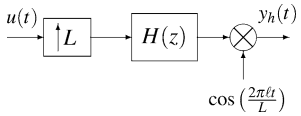

Fig. 2.9 Filtering followed by modulation

Show that (i) the system in Fig. 2.8 is linear but not time invariant, and (ii) $\Psi_s(\omega) = \Psi_u(L\omega)$ and $\Psi_{y_f}(\omega) = \left|F(e^{j\omega})\right|^2 \Psi_u(L\omega)$ where $\Psi(\cdot)$ is PSD.

2.13. Compute impulse responses for BIBO stable systems which admit the following transfer functions:

$$H_1(z) = \frac{2.5}{z^2 + 1.5z - 1}, \quad H_2(z) = \frac{z+1}{z^2 + 3.5z - 2}.$$

2.14. Let $\mathbf{H}(z)$ be a causal transfer function matrix of size $p \times p$. Let $\mathbf{D}(z) = \text{diag}\left(z^{-d_1}, z^{-d_2}, \ldots, z^{-d_p}\right)$ with $d_i \geq 0$ integers. Show that $\tilde{\mathbf{H}}(z) = \mathbf{D}(z)^{-1}\mathbf{H}(z)\mathbf{D}(z)$ may not be causal.

2.15. Consider the two systems in Figs. 2.8 and 2.9. Suppose that the impulse responses of $F(z)$ and $H(z)$ are $\{f(t)\}_{t=0}^{n}$ and $\{h(t)\}_{t=0}^{n}$, respectively, where $n > 1$, and ($\ell > 0$ is any integer)

$$f(t) = h(t)\cos\left(\frac{2\pi\ell t}{L}\right). \tag{2.93}$$

(i) Show that for $L > 1$, the two system block diagrams are equivalent, or $y_f(t) = y_h(t)$ for all time t. That is, filtering followed by cosine modulation has the same effect as filtering with cosine-modulated impulse response.
(ii) Show that, if we remove the interpolator, the two signal block diagrams are not equivalent or $y_f(t) \neq y_h(t)$ for at least some time t.

2.16. Consider again the systems in Figs. 2.8 and 2.9 where the impulse responses of $H(z)$ and $F(z)$ are $\{h(t)\}_{t=0}^{n}$ and $\{f(t)\}_{t=0}^{n}$, respectively, satisfying (2.93) and

$$\left|H\left(e^{j\omega}\right)\right| \approx \begin{cases} 1, & |\omega| \leq \pi/5, \\ 0, & \text{elsewhere.} \end{cases}$$

For $L = 5$, $\ell = 1$, and the input PSD

$$\Psi_u(\omega) = |\omega| \quad \text{for} \quad |\omega| \leq \pi,$$

give rough sketches for the output PSDs for $\{y_f(t)\}$ and $\{y_h(t)\}$.

2.17. Suppose that $H(z)$ in (2.39) is stable. Show that (i) it is analytic outside the unit circle, and (ii) $H(z)$ is continuous on the unit circle, i.e., $H(\mathrm{e}^{j\omega})$ is a continuous function of ω. (*Hint:* A transfer function $H(z)$ is analytic at $z = z_0$, if it admits the (continuous) derivative at $z = z_0$).

2.18. Suppose that $\mathbf{H}(z)$ and $\mathbf{G}(z)$ are BIBO stable with impulse response $\{H(t)\}$ and $\{G(t)\}$, respectively. Show that

$$\frac{1}{2\pi}\int_{-\pi}^{\pi} \mathbf{H}\left(\mathrm{e}^{j\omega}\right)\mathbf{G}\left(\mathrm{e}^{j\omega}\right)^{*}\,\mathrm{d}\omega = \sum_{t=-\infty}^{\infty} H(t)G(t)^{*}$$

and conclude (i) the Parseval's relation (2.51), and (ii) if $\mathbf{H}(z)$ is causal and $\mathbf{G}(z)$ is anticausal, then there holds the orthogonality relation

$$\frac{1}{2\pi}\int_{-\pi}^{\pi} \mathbf{H}\left(\mathrm{e}^{j\omega}\right)\mathbf{G}\left(\mathrm{e}^{j\omega}\right)^{*}\,\mathrm{d}\omega = \mathbf{0}.$$

2.19. Suppose that $\mathbf{H}(z)$ is BIBO stable. Show that $\mathbf{H}(z) = \mathbf{H}_A(z) + \mathbf{H}_C(z)$ with $\mathbf{H}_A(z)$ anticausal, $\mathbf{H}_C(z)$ causal, and

$$\|\mathbf{H}\|_2^2 = \|\mathbf{H}_A\|_2^2 + \|\mathbf{H}_C\|_2^2.$$

2.20. Prove Theorem 2.7.

2.21. (i) If there exists a square polynomial matrix $\mathbf{R}(z)$ such that

$$\mathbf{M}(z) = \mathbf{R}(z)\mathbf{M}_{\mathrm{c}}(z), \quad \mathbf{N}(z) = \mathbf{R}(z)\mathbf{N}_{\mathrm{c}}(z),$$

where $\det(\mathbf{R}(z)) = 0$ for some $z \in \mathbb{C}$, show that $\{\mathbf{M}(z), \mathbf{N}(z)\}$ is not left coprime. If $\mathbf{R}(z)$ is the GCD, show that $\{\mathbf{M}_{\mathrm{c}}(z), \mathbf{N}_{\mathrm{c}}(z)\}$ is left coprime.

(ii) If there exists a square polynomial matrix $\tilde{\mathbf{R}}(z)$ such that

$$\tilde{\mathbf{M}}(z) = \tilde{\mathbf{M}}_{\mathrm{c}}(z)\tilde{\mathbf{R}}(z), \quad \tilde{\mathbf{N}}(z) = \tilde{\mathbf{N}}_{\mathrm{c}}(z)\tilde{\mathbf{R}}(z),$$

where $\det(\tilde{\mathbf{R}}(z)) = 0$ for some $z \in \mathbb{C}$, show that $\{\tilde{\mathbf{N}}(z), \tilde{\mathbf{M}}(z)\}$ is not right coprime. If $\tilde{\mathbf{R}}(z)$ is the GCD, show that $\{\tilde{\mathbf{N}}_{\mathrm{c}}(z), \tilde{\mathbf{M}}_{\mathrm{c}}(z)\}$ is right coprime.

2.22. Find the relation between the two IIR models in (2.54) and (2.66), and draw a similar block diagram to the one in Fig. 2.2 for the state-space realization in (2.67) with $n = 3$.

2.23. Extend the realization in (2.68) (canonical controller form) to cover the MIMO IIR model (2.58) by assuming that $\tilde{M}_0 = I_m$, $\tilde{N}_0 = \mathbf{0}$, and $\ell = \max\{\tilde{n}_\nu, \tilde{n}_\mu\}$.

2.24. Consider a 2×2 MIMO IIR model

$$\mathbf{H}(z) = \frac{z^{-1}}{3 + 2.5z^{-1} + 0.5z^{-2}} \begin{bmatrix} 3(z^{-1}+2) & 6(1+0.5z^{-1}) \\ 3z^{-1} & 3(1+0.5z^{-1}) \end{bmatrix}.$$

(i) Find an ARMA description in the form of (2.57) and the corresponding IIR in the form of left fraction.

(ii) Show that a right fraction is given by

$$\mathbf{H}(z) = \begin{bmatrix} z^{-2} + 2z^{-1} & 2z^{-1} \\ z^{-2} & z^{-1} \end{bmatrix} \begin{bmatrix} 1 + \frac{2.5}{3}z^{-1} + \frac{1}{6}z^{-2} & 0 \\ 0 & 1 + \frac{1}{3}z^{-1} \end{bmatrix}^{-1}$$

which is coprime.

(iii) Compute poles and zeros of $\mathbf{H}(z)$.

(iv) Show that with

$$A = \begin{bmatrix} -\frac{2.5}{3} & -\frac{1}{6} & 0 \\ 1 & 0 & 0 \\ 0 & 0 & -\frac{1}{3} \end{bmatrix}, \quad B = \begin{bmatrix} 1 & 0 \\ 0 & 0 \\ 0 & 1 \end{bmatrix}, \quad C = \begin{bmatrix} 2 & 1 & 2 \\ 1 & 0 & 1 \end{bmatrix},$$

and $D = \mathbf{0}_{2\times 2}$, (A, B, C, D) is a minimal realization.

2.25. (i) Find a right coprime fraction for

$$\mathbf{H}_1(z) = \begin{bmatrix} 1 - z^{-2} \\ 1 - 3z^{-1} + 2z^{-2} \end{bmatrix} \frac{2}{1 - 1.8z^{-1} + 0.8z^{-2}}.$$

(ii) Find a left coprime fraction for

$$\mathbf{H}_2(z) = \frac{2}{1 + 0.4z^{-1} - 0.6z^{-2}} \begin{bmatrix} 2 + 3z^{-1} + z^{-2} & 1 - z^{-2} \end{bmatrix}.$$

(iii) Find minimal realizations for $\mathbf{H}_1(z)$ and $\mathbf{H}_2(z)$. (*Hint:* Use canonical controller form.)

2.26. (i) For an LTV system with impulse response $\{h(t;\tau)\}$, show that it is BIBO stable, if and only if

$$\sum_{\tau=-\infty}^{\infty} |h(t;\tau)| < \infty \quad \forall\, t.$$

(ii) Prove the similar result in (2.76) for MIMO systems.

2.27. Let $|a| > 1$ and $|b| < 1$. Consider state-space model

$$\mathbf{x}(t+1) = A_t \mathbf{x}(t), \quad A_t = \begin{cases} \begin{bmatrix} 0 & a \\ ba^{-1} & 0 \end{bmatrix}, & \text{if } t \text{ is even}, \\ \begin{bmatrix} 0 & ba^{-1} \\ a & 0 \end{bmatrix}, & \text{if } t \text{ is odd}. \end{cases}$$

(a) Compute eigenvalues of A_t and verify that $\rho(A_t) < 1 \; \forall \, t$. (b) Show that

$$\mathbf{x}(t) = \begin{cases} \begin{bmatrix} (b/a)^{2k} & 0 \\ 0 & a^{2k} \end{bmatrix} \mathbf{x}(0), & \text{if } t = 2k, \\ \begin{bmatrix} 0 & a^{2k+1} \\ (b/a)^{2k+1} & 0 \end{bmatrix} \mathbf{x}(0), & \text{if } t = 2k+1. \end{cases}$$

That is, $\|\mathbf{x}(t)\| \to \infty$ as $t \to \infty$, if the second element of $\mathbf{x}(0)$ is nonzero.

2.28. Consider the signal model as in Fig. 2.4, where the noise is AWGN with zero mean and variance σ_v^2. Suppose that the binary data source $\{s(t)\}$ is not equal probable and has probability distribution

$$P_S[s(t) = +1] = p > 0, \quad P_S[s(t) = -1] = 1 - p > 0,$$

and thus, $\mathrm{E}\{|s(t)|^2\} = 1$. Modify the detection rule in (2.85) as

$$\hat{s}(t) = \begin{cases} +1, & \text{if } r(t) > \rho, \\ -1, & \text{if } r(t) < \rho, \end{cases}$$

with ρ a threshold. Then the BER is a function of ρ. Show that

$$\rho = \rho_{\text{opt}} = \frac{\sigma_v^2}{2} \log_e \left(\frac{1-p}{p} \right)$$

minimizes the BER. It is noted that for equal probable case, $\rho_{\text{opt}} = 0$ which coincides with the detection rule (2.85). (*Hint:* Show that

$$\varepsilon_{\text{b}} = (1-p) P_{R|S}[r(t) > \rho \,|\, s(t) = -1] + p P_{R|S}[r(t) < \rho \,|\, s(t) = +1]$$

is a function of ρ. Find its expression and then compute its minimum).

http://www.springer.com/978-1-4614-2280-8

Discrete-Time Linear Systems
Theory and Design with Applications
Gu, G.
2012, XVI, 452 p., Hardcover
ISBN: 978-1-4614-2280-8